LIMNOLOGY
and
OCEANOGRAPHY

ASLO

Limnol. Oceanogr. 00, 2017, 00–00

doi: 10.1002/lno.10590

Differential effects of nitrate, ammonium, and urea as N sources for microbial communities in the North Pacific Ocean

I. N. Shilova ,[1,a] M. M. Mills,[2] J. C. Robidart,[3] K. A. Turk-Kubo,[1] K. M. Björkman,[4] Z. Kolber,[1] I. Rapp,[5] G. L. van Dijken,[2] M. J. Church,[4,b] K. R. Arrigo,[2] E. P. Achterberg,[5] J. P. Zehr[1]*

[1]University of California Santa Cruz, Santa Cruz, California
[2]Stanford University, Stanford, California
[3]National Oceanography Centre, Southampton, United Kingdom
[4]University of Hawaii at Manoa, Honolulu, Hawaii
[5]GEOMAR Helmholtz Centre for Ocean Research, Kiel, Germany

Abstract

Nitrogen (N) is the major limiting nutrient for phytoplankton growth and productivity in large parts of the world's oceans. Differential preferences for specific N substrates may be important in controlling phytoplankton community composition. To date, there is limited information on how specific N substrates influence the composition of naturally occurring microbial communities. We investigated the effect of nitrate (NO_3^-), ammonium (NH_4^+), and urea on microbial and phytoplankton community composition (cell abundances and 16S rRNA gene profiling) and functioning (photosynthetic activity, carbon fixation rates) in the oligotrophic waters of the North Pacific Ocean. All N substrates tested significantly stimulated phytoplankton growth and productivity. Urea resulted in the greatest (>300%) increases in chlorophyll *a* (<0.06 μg L^{-1} and ~0.19 μg L^{-1} in the control and urea addition, respectively) and productivity (<0.4 μmol C L^{-1} d^{-1} and ~1.4 μmol C L^{-1} d^{-1} in the control and urea addition, respectively) at two experimental stations, largely due to increased abundances of *Prochlorococcus* (Cyanobacteria). Two abundant clades of *Prochlorococcus*, High Light I and II, demonstrated similar responses to urea, suggesting this substrate is likely an important N source for natural *Prochlorococcus* populations. In contrast, the heterotrophic community composition changed most in response to NH_4^+. Finally, the time and magnitude of response to N amendments varied with geographic location, likely due to differences in microbial community composition and their nutrient status. Our results provide support for the hypothesis that changes in N supply would likely favor specific populations of phytoplankton in different oceanic regions and thus, affect both biogeochemical cycles and ecological processes.

Nitrogen (N) is a major component of cell constituents, including proteins and nucleic acids, and is considered the primary limiting element for phytoplankton growth and photosynthetic carbon fixation in oligotrophic oceans (Eppley et al. 1977; Graziano et al. 1996; Mills et al. 2004; Moore et al. 2013). While there is an intricate balance among iron (Fe), phosphorus (P), and N in shaping microbial communities in the marine environment, nutrient enrichment experiments have demonstrated that the availability of N alone can stimulate growth of phytoplankton and affect heterotrophic communities in the oligotrophic ocean (Mills et al. 2004, 2008; Bonnet et al. 2008; Davey et al. 2008; Moore et al. 2008; Ortega-Retuerta et al. 2012).

N actively cycles in the upper ocean where sunlight provides energy that rapidly fuels production and consumption of N compounds. The major forms of N in the surface ocean include dinitrogen gas (N_2), ammonium (NH_4^+), nitrate (NO_3^-), nitrite (NO_2^-), and dissolved organic N (DON). N_2 fixation can account for 40–50% of net community production in the North Pacific Subtropical Gyre (NPSG) (Böttjer et al. 2016), however, net community production in this ecosystem is less than 10% of gross primary production (Quay

*Correspondence: zehrj@ucsc.edu

[a]Present address: Second Genome, Inc, South San Francisco, CA

[b]Present address: Flathead Lake Biological Station, University of Montana, Polson, Montana

I. S. and M. M. have contributed equally to this work.

Additional Supporting Information may be found in the online version of this article.

et al. 2010). Although abundant, the bulk of the DON pool, except urea, amino acids, and nucleotides, generally does not appear readily bioavailable and is believed to be minor source of N for most phytoplankton (Aluwihare and Meador 2008; Mulholland and Lomas 2008). The major fixed N pools (NH_4^+, NO_3^-, NO_2^-, urea) have different sources and rates of production and turnover. Regeneration by heterotrophic bacteria, and excretion and release by zooplankton, are the major natural sources of NH_4^+ and urea in the upper ocean (Corner and Newell 1967; Mayzaud 1973; Mitamura and Saijo 1981; Bidigare 1983; Hansell and Goering 1989; Bronk et al. 1998). Regenerated production supported by this rapidly recycled N accounts for over 90% of gross primary production in the oligotrophic oceans (Eppley and Peterson 1979). NO_3^- is supplied to the euphotic zone predominately via mixing or upwelling of sub-euphotic zone waters with additional contributions derived from nitrification within the euphotic zone (Dore and Karl 1996; Yool et al. 2007) and atmospheric deposition (Duce et al. 2008). N from sources external to the surface ocean supports "new" production, which balances N export losses due to sinking to the deep ocean (Dugdale and Goering 1967). New N is also introduced through N_2 fixation carried out by diazotrophs, a small subset of the marine microbial community (Dugdale and Goering 1967; Zehr and Kudela 2011). Recycling of diazotroph organic matter transfers this new N to the dissolved pool as DON (e.g., amino acids and urea) and/or NH_4^+ where it can be used to fuel primary production (Montoya et al. 2002; Zehr and Kudela 2011). Thus, the chemical form of N is an important factor in the functioning of ocean ecosystems.

Microbial communities that utilize dissolved N in oligotrophic oceans are diverse, but are comprised largely of cyanobacteria (*Prochlorococcus* and *Synechococcus*), diatoms, eukaryotic picoplankton (for example, prymnesiophytes and pelagophytes) and a variety of heterotrophic bacteria (including *Pelagibacter ubique*) and Archaea (Waterbury et al. 1979; Chisholm et al. 1988; DuRand et al. 2001; Karner et al. 2001; Morris et al. 2002; Worden et al. 2004). These microorganisms have a variety of N assimilation strategies that differ in the rates of N uptake and assimilation, regulation of N metabolism, and their abilities to use different N forms. For example, N-limited Low Light (LL) *Prochlorococcus* strains appear unable to grow on NO_3^- (Moore et al. 2002), while some strains of the High Light (HL) ecotypes are able to assimilate NO_3^-, although at reduced rates of growth relative to other substrates (e.g., NH_4^+, Martiny et al. 2009; Berube et al. 2015). Many marine microorganisms use NO_3^- as a source of N, including diatoms and *Synechococcus*, as well as some heterotrophic bacteria (Allen et al. 2001, 2006; Casey et al. 2007; Collier et al. 2012). Isotopic analyses suggest that eukaryotic phytoplankton smaller than 30 μm in the Sargasso Sea acquire a major fraction of their N demand from NO_3^- (Fawcett et al. 2011). The assimilation of urea by phototrophic and heterotrophic marine microorganisms is common across numerous phylogenetic groups and ecological niches (McCarthy 1972*a*,*b*; Hallam et al. 2006; Baker et al. 2009; Collier et al. 2009; review by Solomon et al. 2010). Many *Prochlorococcus* strains and all tested *Synechococcus* strains can utilize urea, yet this N substrate supports different growth rates within each genus (Moore et al. 2002). Moreover, rates of urea uptake and assimilation in natural microbial populations appear comparable to those of NH_4^+ (Sahlsten 1987; Price and Harrison 1988), although rates differ among phytoplankton taxa (Lomas and Glibert 2000; Moore et al. 2002; Fan et al. 2003). Despite the accumulated knowledge about N utilization by marine microorganisms, taxon-specific preferences and utilization efficiencies for different N species are still ambiguous, especially in the oligotrophic open ocean.

The form and supply of different N substrates are important controls on microbial community composition. Understanding the effect of different N forms is critical because N supply to the surface oceans will likely change due to greater stratification caused by climate change (Gruber and Galloway 2008; Capotondi et al. 2012; Kim et al. 2014), and the projected increase in atmospheric anthropogenic N deposition (Duce et al. 2008). We performed nutrient enrichment experiments to determine the functional and taxonomic responses in microbial communities to different N forms and whether the responses vary depending on the nutrient status (mesotrophic vs. oligotrophic) in the North Pacific Ocean. The measured functional responses included CO_2 fixation rates and changes in chlorophyll *a* (Chl *a*) and photosynthetic parameters. The taxonomic responses were assessed by quantifying the abundance of major phytoplankton groups and heterotrophic bacteria as well as assessing relative shifts in cyanobacterial and heterotrophic community composition based on 16S rRNA gene sequencing.

Materials and methods

Nutrient amendments experiments

Experiments were conducted in August of 2014 during the Nitrogen Effects on Marine microOrganisms cruise (NEMO, R/V *New Horizon*) at two sites in the North Pacific Ocean: one within the western part of the transitional zone of the California Current System (CCS; Station 38, hereafter referred to as TZ), and one in the oligotrophic NPSG (Station 52, hereafter referred to as GY: Fig. 1). The TZ site was in an anticyclonic eddy, based on the sea surface height anomaly (Fig. 1b). The two sites were chosen based on a priori assumptions of nutrient limitation of primary productivity at each site. The availability of Fe can play an important role in controlling phytoplankton growth in the CCS (Biller and Bruland 2014). In contrast, N was assumed to be limiting primary productivity in the NPSG. All experiments were undertaken using strict trace-metal clean techniques (Mills et al. 2004) during the preparation and sampling of the experiments. Water at each station was collected from 25 m depth

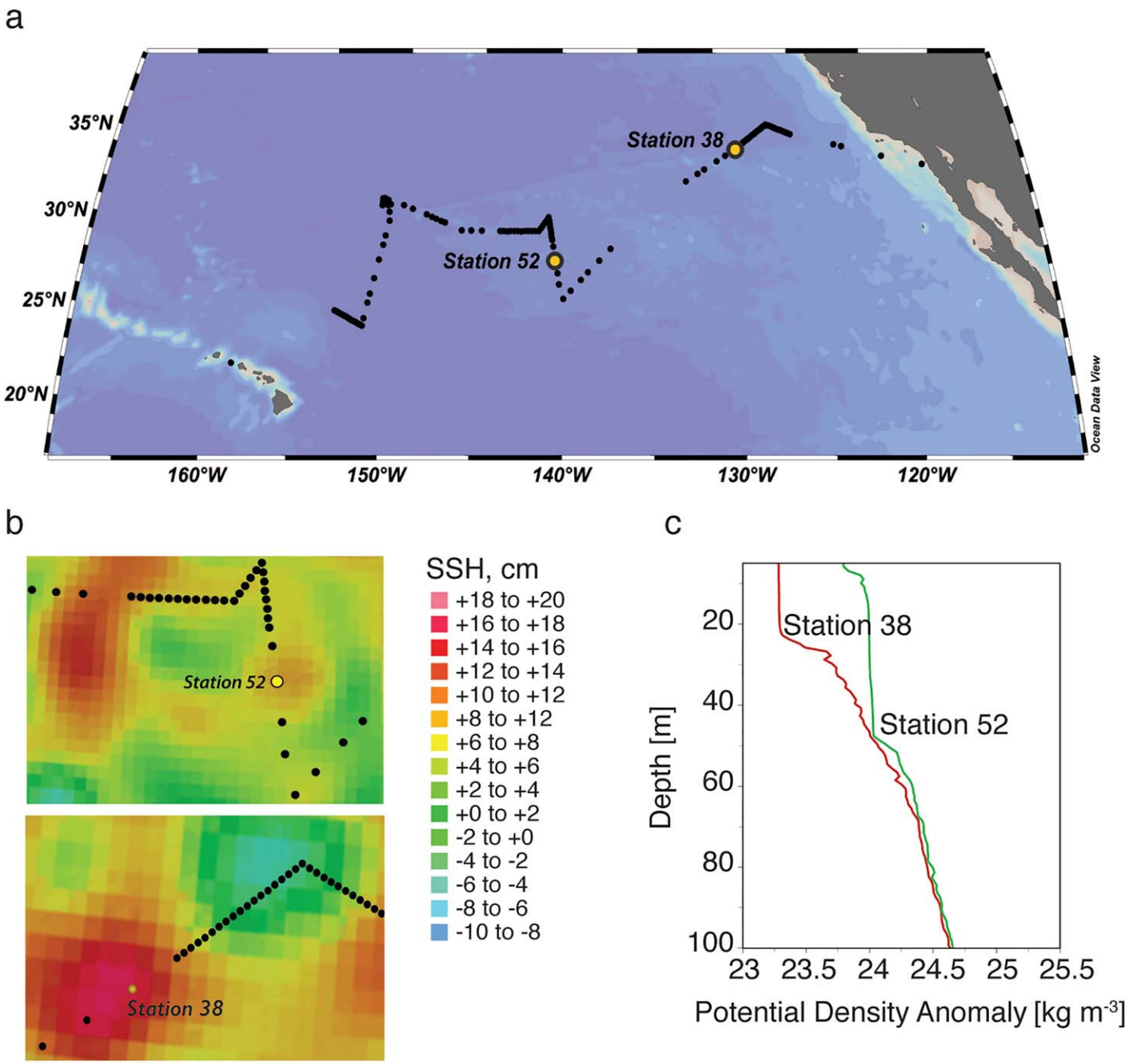

Fig. 1. Geographic locations in the North Pacific (**a**), sea surface height anomaly (**b**), and potential density profiles (**c**) of the two stations where nutrient addition experiments were conducted in August of 2014. Station 38 was in the western part of the transition zone of the California Current System (station TZ), and Station 52 was in the oligotrophic North Pacific Subtropical Gyre (station GY).

using a towed fish with Teflon diaphragm pump. The water was pumped gently into a 40 L carboy in a trace-metal clean laboratory van. This allowed mixing of the seawater before it was distributed into incubation bottles. Seawater was subsampled into 4 L polycarbonate bottles (Thermo Scientific™ Nalgene™) that had been acid-washed and, prior to the experiment, rinsed thoroughly with seawater at the site of each experiment. The bottles used in the first experiment were acid-rinsed and reused for the same treatments in the second experiment. In the TZ site experiment, triplicate incubation bottles were amended with either NO_3^- (final concentration 5.0 μmol L^{-1}), NH_4^+ (final concentration 5.0 μmol L^{-1}), urea (final concentration 5.0 μmol N L^{-1}), 0.2 μm pre-filtered deep (600 m) seawater (FDW) (12.5% of total volume, equivalent to ~5 μmol L^{-1} NO_3^- addition), Fe^{3+}(final concentration 2 nmol L^{-1}) or a combined treatment

containing NO_3^- and Fe^{3+} (final concentrations of 5 μmol L^{-1} and 2 nmol L^{-1}, respectively). The Fe and $Fe + NO_3^-$ treatments were used to test for Fe and $Fe + NO_3^-$ co-limitation. The GY experiment was similar in design with the exception that all N compounds were added to achieve a final concentration of 2.5 μmol N L^{-1}, and 6% of total volume of FDW was added (an approximately 2.5 μmol L^{-1} NO_3^- addition). The N additions in the TZ experiment were higher than in the GY experiment based on previous work in the CCS by Biller and Bruland (2014) who measured residual NO_3^- concentrations in the transitional zone of CCS ranging from 5 μmol L^{-1} to 15 μmol L^{-1}, while residual NO_3^- at the GY was negligible (<10 nmol L^{-1}). In both experiments, the Controls consisted of triplicate bottles filled with unamended seawater from the respective station and depth. The Controls were incubated and processed in the same manner as the experimental treatments. All nutrient additions were undertaken in a laminar flow hood. The nutrient solutions, except the Fe solution, were passed through Chelex100 to minimize trace metal contamination. Purity controls were measured for all stocks to ensure the absence of contamination (i.e., Fe stocks did not contain dissolved N, N stocks did not contain Fe, and individual N stocks were not contaminated with other N species). Incubation bottles were placed in a flow-through surface seawater incubator, to achieve surface ocean temperatures during the experiment, with neutral screening to attenuate incident light to approximately 35% of the surface solar irradiance. The setup and samplings of the setup (T0), and at 24 (T24) and 48 (T48) h after the start of the incubation were undertaken before dawn. Rates of primary productivity and concentrations of Chl *a* and nutrients were measured in samples immediately after the nutrient amendments (T0) and at T48. Samples for photophysiological parameters, cell abundance, and microbial community composition were collected prior to the nutrient amendments (T0), at T24, and T48.

Nutrient analysis

Samples for subsequent analyses of nutrient concentrations were collected in acid-washed, sample rinsed polyethylene bottles and stored frozen at −20°C until analyzed (Dore et al. 1996). $NO_3^- + NO_2^-$, soluble reactive phosphorus (SRP) and $Si(OH)_4$ concentrations (μmol L^{-1}) were determined using a segmented flow continuous flow automated nutrient analyzer (SEAL Analytical - AA3) using standard colorimetric techniques (Strickland and Parsons 1972). Accuracy of each analysis was checked using WAKO the International Cooperative Study of the Kuroshio and Adjacent Regions (CSK) and Ocean Scientific International Ltd. (OSIL) reference materials. $NO_3^- + NO_2^-$ concentrations < 500 nmol L^{-1} were determined using the high-sensitivity chemiluminescence technique (Garside 1982; Dore and Karl 1996) with a detection limit of 1 nmol L^{-1}. NH_4^+ samples were measured using the SEAL AA3 coupled with a 2 m liquid waveguide capillary cell, employing indophenol blue chemistry (Li et al. 2005; Zhu et al. 2014). The limit of detection for this method is 4 nmol L^{-1}.

Samples for subsequent analyses of trace metal concentrations were collected using an acid-cleaned hose (polyvinyl chloride, PVC) attached to a plastic-coated steel cable and lowered to the desired collection depth (25 m). Water was pumped to the surface using a Teflon bellows pump (Almatec A15) and transferred, entirely enclosed, into a trace-metal clean sampling container located in an on-deck trace-metal clean lab. Samples for the determination of dissolved Fe concentrations were filtered through a 0.2 μm Sartobran 300 capsule filter (Sartobran 300, Sartorius), collected in acid-cleaned 125 mL low density polyethylene (LDPE, Nalgene) bottles, and immediately acidified with 150 μL hydrochloric acid (~11 mol L^{-1} HCl, OPTIMA grade, Fisher Scientific) to a final pH of 1.9. Dissolved Fe samples from the incubation experiments were collected at T0 and T48. The samples were filtered using 0.45 μm polycarbonate membrane filters (Millipore) mounted in an acid cleaned filter holder (Swinnex, Millipore), acidified to pH 1.9. and analyzed on-board ship using flow injection analysis (FIA). Dissolved Fe was determined on-board the ship using luminol chemiluminescence by flow injection analysis (FIA) following Obata et al. (1993). The FIA system was equipped with a Toyopearl AF Chelate 650M resin. Sample concentrations were determined by standard addition and were verified by analyzing "Sampling and Analysis of Fe (SAFe)" reference seawater with each analytical run. Our results for the reference seawater were in good agreement with the consensus values for SAFe S: 0.090 ± 0.008 nmol L^{-1} ($n = 2$) and SAFe D2: 1.043 ± 0.004 nmol L^{-1} ($n = 2$). The precision of the method varied between 4% and 8% (1 SD) and was determined by analyzing internal reference seawater after every 10 samples. The blank of the FIA method was 0.028 ± 0.010 nmol L^{-1} ($n = 12$) and the limit of detection (LOD) determined by the product of the blank and three times standard deviation of the blank was 0.058 nmol L^{-1}.

Chlorophyll *a*

Subsamples (300 mL or 400 mL) were collected from each of the triplicate bottles and filtered through 25 mm diameter glass fiber filters (GF/F, Whatman). Filters were placed in 5 mL of 90% acetone and extracted in the dark at 2°C for 24 h. Samples were equilibrated to room temperature before measurement. Fluorescence at 685 nm was measured using a Turner Designs TD-700 Field Fluorometer, calibrated with a Chl *a* standard (Sigma-Aldrich, C6144) dissolved in 90% acetone using the Welschmeyer (1994) filter setup.

^{14}C-based primary productivity

Primary productivity (PP) was determined using ^{14}C-labelled bicarbonate as a tracer for net inorganic carbon fixation (Steeman-Nielsen 1952). A subsample from each treatment bottle was collected into acid-cleaned, sample-rinsed

75 mL polycarbonate bottles and spiked with ^{14}C-bicarbonate to achieve a final activity of approximately 250 μCi L^{-1} (or 9.3 MBq L^{-1}, MP Biomedical #017441H). The bottles were incubated from dawn to dusk in the same on-deck incubator previously described. At the end of the daylight period, the entire sample volume was filtered through a 25 mm GF/F. The filters were placed into 20 mL borosilicate scintillation vials, acidified (1 mL, 2 mol L^{-1} hydrochloric acid) and vented for 24 h prior to the addition of scintillation cocktail (Ultima Gold LLT, Perkin-Elmer). Radioactivity was determined by liquid scintillation counting. Subsamples (250 μL) for total ^{14}C-radioactivity were collected from each incubation bottle and fixed in phenethylamine (Sigma-Aldrich #407267). Rates of carbon fixation are expressed as μmol C L^{-1} d^{-1}.

Active fluorescence

Fast Repetition Rate Fluorometry (FRRF) was utilized to evaluate possible changes in photophysiology in response to the availability of different N and Fe substrates, as described in Kolber et al. (1998). The FRRF instrument was operated with multiple excitation wavelengths (450 nm, 470 nm, 505 nm, and 530 nm) that allowed for the rapid assessment of photosystem II (PSII) physiology in different groups of phytoplankton. Samples (500 mL) were first dark adapted (20 min) before conducting fluorescence measurements. Fluorescence transients were acquired in samples that were continuously recirculated through the instrument sample chamber. The sample chamber was exposed to FRRF excitation protocol composed of a series of microsecond-long flashlets of controlled excitation power. The saturation phase of the excitation was comprised of 100 flashlets at 2.5 microsecond intervals. With the pulse excitation power of 30,000–50,000 μmol quanta m^{-2} s^{-1}, the rate of excitation delivery to PSII centers far exceeded the capacity of photosynthetic electron transport between PSII and PSI. This resulted in a progressive saturation of the observed fluorescence transients within the first 40–60 flashlets, with a rate proportional to the functional absorption cross section at particular wavelength. The saturation phase was followed by 90 flashlets applied at exponentially increasing time interval starting at 20 μs, over a period of 250 ms. As the average excitation power decreased, the fluorescence signal relaxed with a kinetics mostly defined by the rates of electron transport between PSII and PSI. Each sample measurement consisted of an average of 32 transients, and each sample was measured three times at each wavelength. Blanks were obtained by gently filtering sample water through a 0.2 μm syringe filter and processing it in the same manner as the samples. Recorded fluorescence transients were processed with FRRF software (http://soliense.com/) to estimate PSII maximum in vivo fluorescence (Fm), maximum photochemical efficiency (Fv/Fm), the functional absorption cross section (σ_{PSII}) for all Chl *a*-containing cells (excitation wavelength of 470 nm) and phycoerythrin-containing plankton (e.g., *Synechococcus*, excitation wavelength of 505 nm), and the kinetics of the PSII-PSI electron transport.

Flow cytometry

Samples (2 mL of seawater) for subsequent flow cytometric enumeration of picoplankton were immediately fixed with glutaraldehyde (0.25% v/v final concentration) upon collection, kept at room temperature in the dark for 15 min, then flash frozen and kept at −80°C until processing. Abundances of *Prochlorococcus*, *Synechococcus*, photosynthetic picoeukaryotes (PPEs), and heterotrophs were enumerated using a BD Biosciences Influx Cell Sorter (BD Biosciences, San Jose, California, U.S.A.) equipped with a 488 nm Sapphire laser (Coherent, Santa Clara, California, U.S.A.) using a 70 μm nozzle. All fixed seawater samples were pre-filtered using a CellTrics® filter with 30 μm mesh (Partec, Swedesboro, New Jersey, U.S.A.). *Synechococcus* populations were identified based on the presence of phycoerythrin (orange fluorescence; 572–27 photomultiplier tube, PMT) and all other non-phycoerythrin populations were identified using forward scatter (FSC) as a proxy for cell size and Chl *a* content (red fluorescence; 692–20 PMT). To enumerate non-pigmented cells (heterotrophs), samples were stained with SYBR® Green I nucleic acid stain (Lonza, Allendale, New Jersey, U.S.A.) according to the protocol described in Marie et al. (1999). To determine the abundances of non-pigmented heterotrophs with High Nucleic Acid content (HNA cells), the abundance of *Prochlorococcus* and *Synechococcus* cells were subtracted from all HNA cells. Data collection was triggered in the forward scatter (FSC) channel for photosynthetic cells and in the green channel (531-40 PMT) for SYBR-stained cells. Photosynthetic cells were counted for 10 min; SYBR-positive cells were counted for 1.5 min. Cell counts were processed in FlowJo v10.0.7 (Tree Star, Ashland, Oregon, U.S.A.).

DNA extraction

One to two liters of seawater from each incubation bottle was filtered onto 0.2 μm Supor membrane filters (Pall Corp., Ann Arbor, Michigan, U.S.A.) using peristaltic pumps. The filters were placed in sterile 2.0 mL microcentrifuge tubes containing 0.5 mm and 1 mm diameter glass beads (Biospec, Bartlesville, Oklahoma, U.S.A.), flash frozen in liquid N_2, and stored at −80°C until DNA extraction. DNA was extracted using the Qiagen DNeasy Plant kit (Valencia, California, U.S.A.), with modifications outlined in Moisander et al. (2008) to improve recovery of high quality DNA. The final wash steps and DNA elution were automated using a QIAcube robotic workstation (Qiagen). DNA quantity and quality was measured using a NanoDrop (Thermo Scientific, Waltham, Massachusetts, U.S.A.) with an average DNA yield 1100 ± 900 ng L^{-1} seawater.

16S rRNA gene sequencing and sequence read processing

Community composition was analyzed based on sequences of the V3-V4 hypervariable region of the 16S rRNA gene

using universal primers targeting Bacteria, Bakt_341F, and Bakt_805R (Herlemann et al. 2011). Primers were modified with common sequence linkers (Moonsamy et al. 2013) to facilitate library preparation. PCR amplifications were carried out in triplicate 25 μL reactions for each sample, with the following reaction conditions: 1X Platinum Taq PCR buffer – Mg (Invitrogen, Carlsbad, California), 2.5 mmol L^{-1} $MgCl_2$, 200 μmol L^{-1} dNTP mix, 0.25 μmol L^{-1} of both forward and reverse primers, 3 U Platinum Taq DNA Polymerase (Invitrogen), and 1 μL of the DNA template. DNA was amplified using the following thermocycling conditions: initial denaturation at 95°C for 5 min, 25 cycles of denaturation at 95°C for 40 s, annealing at 53°C for 40 s, elongation at 72°C for 60 s, and a final elongation at 72°C for 7 min. Pooled amplicons underwent 10 more amplification cycles to add sequencing adaptors and sample-specific barcodes at the DNA Services Facility at the University of Illinois, Chicago, using the targeted amplicons sequencing approach described in Green et al. (2015). After the second round of PCR amplification performed by DNA Services at UIC, library concentrations were equalized using SequalPrep purification plates (ThermoFisher Scientific). Paired-end reads were sequenced at the W.M. Keck Center for Comparative and Functional Genomics at the University of Illinois at Urbana-Champaign using Illumina MiSeq technology. Sequences of the 16S rRNA gene amplicons were obtained from a total of 91 samples that included samples in three replicates from T0, T24, and T48 for both experiments. There were on average 9986 reads per sample (median = 9990, minimum = 9664, and maximum = 10,340 reads per sample). De-multiplexed raw paired-end reads were merged using PEAR (Zhang et al. 2014). Assembled sequences were then quality filtered (split_libraries_fasta.py; phred score of 20) and chimeras were removed using a de novo approach (identify_chimeric_seqs.py) in QIIME (Caporaso et al. 2010). Operational taxonomic units (OTU) were defined at 99% nucleotide similarity using the usearch6.1 clustering method (Edgar 2010; pick_otus.py) and representative sequences were retrieved (pick_rep_set.py) in QIIME. The taxonomy of representative sequences was assigned using a Greengenes reference database (http://greengenes.secondgenome.com/downloads/database/13_5; DeSantis et al. 2006), and the assign_taxonomy.py QIIME script. We used the default parameters for the uclust consensus taxonomy assigner through QIIME (the minimum percent similarity for a taxonomic assignment was 0.9). The 16S rRNA gene sequences were deposited in Sequence Read Archive at National Center for Biotechnology Information (NCBI, http://www.ncbi.nlm.nih.gov/sra) under BioProject accession number PRJNA358607.

Oligotyping

The oligotyping approach separates individual taxa, "oligotypes," within closely related organisms based on high entropy nucleotide positions in the 16S rRNA gene sequence (Eren et al. 2013). In order to define oligotypes for *Prochlorococcus* and *Synechococcus*, we used the oligotyping pipeline version 2.0 (27 May 2015) and followed the instructions available at http://oligotyping.org (Eren et al. 2013). The oligotyping analysis was performed separately for both *Prochlorococcus* and *Synechococcus*. A total of 395,666 and 10,271 reads were obtained for *Prochlorococcus* and *Synechococcus*, respectively, from samples taken at T0 and T48 in the two experiments. Before the oligotyping analysis, the sequences were aligned using PyNAST (Caporaso et al. 2010) and Greengenes 16S rRNA gene reference database (gg_13_5 version available at http://greengenes.secondgenome.com/). Shannon entropy calculations were followed by the oligotyping analysis, which was run until each oligotype had converged (as described in Eren et al. 2013). The following parameters were chosen for both *Prochlorococcus* and *Synechococcus* oligotyping analyses: $a = 0.1$ and $s = 2$, where "a" is the minimum percent abundance of an oligotype in at least one sample and "s" is the minimum number of samples where an oligotype is expected to be present (Eren et al. 2013). The minimum substantial abundance criterion, M, determines the minimum abundance of the most abundant unique sequence in an oligotype and helps to reduce noise (Eren et al. 2013). For *Prochlorococcus* and *Synechococcus* oligotyping analyses, M was 100 and 20, respectively. To assign taxonomy, the representative sequences of the oligotypes were searched against the reference genome database at NCBI using blastn version 2.3.0+ (Altschul et al. 1990). The BLAST search was done with the default parameters, and all best hits were saved. Because some strains within the genera *Prochlorococcus* and *Synechococcus* have identical 16S rRNA V3-V4 region sequences, a representative sequence of an oligotype often was equally identical to several strains. We called a group of such identical strains an eStrain, and the strains within each eStrain are reported in Supporting Information Table S1. Note that the sequences belonging to one oligotype are identical at the selected nucleotide positions within the amplified ~441 nt region, but may vary at other positions within the 16S rRNA gene. Next, the relative abundance of oligotypes was used to calculate the absolute abundance using the cell counts for *Prochlorococcus* and *Synechococcus*, and the absolute numbers were used in further analyses.

Shifts in community composition

The changes in composition of the heterotrophic microbial communities and *Prochlorococcus* and *Synechococcus* communities, were analyzed using the *Phyloseq* package (McMurdie and Holmes 2013) within R (The R Core Team 2013, http://www.r-project.org). For heterotrophic community analysis, phylum "Cyanobacteria" (that includes sequences from chloroplasts) were excluded, and the selected taxa were required to have a minimum of 50 reads total, resulting in 676,090 sequences total in all samples (minimum of 6195, median of 7040, and

Table 1. Initial conditions at the two hydrographic stations where N amendment experiments were conducted.

		GY station	TZ station
Date		29 Aug 14	24 Aug 14
Location	Latitude (ddm)	27.281	33.502
	Longitude (ddm)	−140.382	−129.37
Physics	Temperature, °C	23.84 ± 0.01	19.50 ± 0.04
	Salinity	35.41 ± 0.01	33.47 ± 0.01
Nutrients	$NO_3^- + NO_2^-$, nmol L^{-1}	2.4 ± 0.7	2.5 ± 0.4
	NH_4^+, nmol L^{-1} *	36 ± 10	58 ± 3
	SRP, μmol L^{-1} ***	0.094 ± 0.005	0.272 ± 0.005
	$Si(OH)_4$, μmol L^{-1} ***	1.35 ± 0.02	2.14 ± 0.01
	Fe, nmol L^{-1}	Below LOD‡	Below LOD‡
Phytoplankton activity	Chl *a*, μg L^{-1}	0.058 ± 0.001	0.057 ± 0.003
	^{14}C-PP, μmol C L^{-1} d^{-1}	0.33 ± 0.02	0.34 ± 0.01
	Fm_{470}	3.4 ± 0.2	3.6 ± 0.3
	Fv/Fm_{470} **	0.34 ± 0.02	0.51 ± 0.01
	$\sigma_{PSII\text{-}470} \times 10^{-20}$ m^{-2} $quanta^{-1}$	850 ± 40	900 ± 40
Cell abundances	Phytoplankton total, mL^{-1}	$1.6 \pm 0.5 \times 10^5$	$1.1 \pm 0.5 \times 10^5$
	Prochlorococcus, mL^{-1}	$1.6 \pm 0.5 \times 10^5$ (30.8%)	$1.0 \pm 0.5 \times 10^5$ (20.3%)
	Synechococcus, mL^{-1} *	$1.2 \pm 0.8 \times 10^3$ (0.2%)	$3.9 \pm 0.7 \times 10^3$ (0.8%)
	Photosynthetic picoeukaryotes, mL^{-1} *	$1.14 \pm 0.03 \times 10^3$ (0.2%)	$2.5 \pm 0.2 \times 10^3$ (0.5%)
	HNA cells, mL^{-1}	$1.2 \pm 0.1 \times 10^5$ (23.1%)	$1.3 \pm 0.2 \times 10^5$ (25.3%)
	LNA cells, mL^{-1}	$2.4 \pm 0.2 \times 10^5$ (46.2%)	$2.6 \pm 0.3 \times 10^5$ (53.1%)
	Total cells†, mL^{-1}	$5.2 \pm 0.5 \times 10^5$	$5.0 \pm 0.6 \times 10^5$

Concentrations of nutrients are shown as an average (±standard deviation) of three replicates. Chl *a*, chlorophyll *a* concentration; ^{14}C-PP, primary productivity rates; HNA, high nucleic acid cells; LNA, low nucleic acid cells; Fm_{470}, maximum fluorescence at 470 nm; Fv/Fm_{470}, maximum photochemical efficiency of PSII measured at 470 nm; $\sigma_{PSII\text{-}470}$, functional absorption cross-section of PSII measured at 470 nm. Significant difference in means is shown with *** for $p < 0.001$, ** for $p < 0.01$ and * for $p < 0.05$ (two-sample *t*-test).
† Total cells: *Prochlorococcus* + *Synechococcus* + Photosynthetic picoeukaryotes + HNA + LNA cells.
‡ Fe limit of detection (LOD) was 0.058 nmol L^{-1}.

maximum of 9493 sequences per sample). Ecological distances among the samples were estimated with the Bray–Curtis and Jaccard indices. To compare the community shifts, resulting from different treatments, Principal Coordinate Analysis (PCoA) was applied to the distance matrices. In addition, the relative read abundances for heterotrophic microbial communities were standardized to the median sequence depths (rarefied). There was little difference in the depth of sequencing among the samples (maximum difference < 600 reads with a mean of ~10K reads per sample) and the PCoA results for standardized data were similar to the results from the non-standardized data.

Software

All statistical analyses were done in R (The R Core Team 2013, http://www.r-project.org): two-sample *t*-test for comparisons of means for Chl *a*, PP, abundances, and FRRF measurements between treatments and controls and between treatments. To test for the observed differences in community composition among treatments, analysis of similarities was done on the Bray–Curtis dissimilarity distance matrix (*anosim* function within the "vegan" package in R, Oksanen et al. 2016). The statistic *R* in analysis of similarities is based on the difference of mean ranks between the groups and within groups, ranges from −1 to 1, and *R* value of 0 indicates random groupings. In addition to analysis of similarities, analysis of variance (*adonis* function in "vegan") was done on the Bray–Curtis dissimilarity matrix. Data were visualized using the ggplot2 package (Wickham 2009) in R, and all final figures were prepared for publication using Adobe Illustrator.

Results

Initial conditions

The physical and chemical conditions at the two experimental sites differed substantially. TZ (Station 38) was located in the transition zone between the California Current and the NPSG along the eastern margin of an anticyclonic eddy (Fig. 1a,b). GY (Station 52) was located in the oligotrophic waters of the central gyre and further west in the NPSG in an area of relatively low eddy activity (Fig. 1b). Both salinity and seawater temperature were higher at GY

than at TZ (Table 1). The mixed layer depth was twice as deep at GY (48 m) in comparison to TZ (24 m) (Fig. 1c).

Concentrations of $NO_3^- + NO_2^-$ in near-surface waters were low (<3 nmol L^{-1}) at both experimental sites (Table 1) while concentrations of NH_4^+ were higher at TZ (58 ± 3 nmol L^{-1} vs. 36 ± 10 nmol L^{-1} at GY). Soluble reactive phosphorus (SRP) concentrations were approximately 3-fold higher and concentrations of $Si(OH)_4$ were 1.5-fold higher at TZ compared to GY. Finally, surface concentrations of dissolved Fe were below detection (LOD = 0.058 nmol L^{-1}) at both sites.

The abundance of total picoplankton cells was approximately equal at the two experimental stations (Table 1, $4.7 \pm 0.8 \times 10^5$ and $5.0 \pm 0.6 \times 10^5$ cells mL^{-1} at GY and TZ, respectively) but the composition of the communities was somewhat different. Phytoplankton cells were 1.5-fold more abundant at GY relative to TZ (Table 1) mainly due to *Prochlorococcus*; however, the difference was not significant ($1.6 \pm 0.5 \times 10^5$ cells mL^{-1} and $1.0 \pm 0.5 \times 10^5$ cells mL^{-1} at GY and TZ, respectively). *Synechococcus* was approximately 100-times less abundant than *Prochlorococcus* at both sites ($1.2 \pm 0.8 \times 10^3$ and $3.9 \pm 0.7 \times 10^3$ cells mL^{-1} at GY and TZ, respectively). *Synechococcus* abundance was 3-times higher at TZ compared to GY, accounting for 0.8% and 0.2% of total cells at each site, respectively. Likewise, the abundance of photosynthetic picoeukaryotes (PPE) was low at both sites ($1.14 \pm 0.03 \times 10^3$ and $2.5 \pm 0.2 \times 10^3$ cells mL^{-1} at GY and TZ, respectively), with TZ having ~2.3-times more PPE cells than GY. PPE accounted for ≤ 0.5% of the total cell population at both sites. Finally, heterotrophic bacteria were enumerated as either high nucleic acid (HNA)- or low nucleic acid (LNA)-containing populations, the latter of which was more abundant (Table 1). The abundances of HNA and LNA cells were similar between the two sites ($1.2 \pm 0.2 \times 10^5$ and $2.5 \pm 0.3 \times 10^5$ for HNA and LNA cells, respectively).

Despite the differences in physicochemical conditions and the composition of the microbial communities, the initial concentrations of Chl *a* and rates of PP were similar at the two stations (Table 1). In contrast, maximum photochemical efficiency of PSII measured at excitation wavelength of 470 nm (Fv/Fm_{470}) was higher at TZ (0.51 ± 0.01) than at GY (0.34 ± 0.02), while no significant difference was detected between stations with respect to functional absorption cross-section of PSII ($\sigma_{PSII\text{-}470}$).

Phytoplankton Chl *a* concentrations and PP rates

All tested N forms and Fe alone resulted in significant increases in Chl *a* concentrations and rates of PP after 48 h of incubation at both locations, and the response at GY was in general larger than at TZ (Fig. 2). Additional nutrients (for example through the addition of Fe or filtered deep water, FDW) did not enhance the response observed for the N forms further.

The largest increases in concentrations of Chl *a* at TZ after 48 h of incubation were observed in response to urea and NH_4^+ additions (0.19 ± 0.01 μg L^{-1}), >3.5-times higher in comparison to the Control (no nutrient addition, Chl_{cnt}, 0.052 ± 0.002 μg L^{-1}) (Fig. 2a). Addition of NO_3^- increased Chl *a* concentrations by 1.4-fold relative to Chl_{cnt} at TZ. At GY, the urea addition resulted in the largest responses in Chl *a* concentration (0.18 ± 0.01 μg L^{-1}) compared to the Chl_{cnt} (0.034 ± 0.003 μg L^{-1}), followed by the NH_4^+ and NO_3^- additions (3-times higher relative to Chl_{cnt})).

Changes in PP were similar to the Chl *a* responses in both experiments, with 4-times higher carbon fixation rates observed in response to additions of urea and NH_4^+ at TZ (1.40 ± 0.07 μmol C L^{-1} d^{-1}) and 8-times higher rates in response to urea at GY (1.3 ± 0.1 μmol C L^{-1} d^{-1}) in comparison to the Controls at 48 h (PP_{cnt}; Fig. 2b). The NO_3^- addition at TZ resulted in 2.5-times higher PP rates relative to the PP_{cnt}. Both NH_4^+ and NO_3^- yielded > 5-times higher PP relative to the PP_{cnt} after 48 h of incubation at GY.

In addition to stimulation by N substrates, the Fe addition alone produced a significant increase in Chl *a* concentrations (40% increase over Chl_{cnt}) and rates of PP (>20% increase over PP_{cnt}) at both locations after 48 h of incubation (Fig. 2; Supporting Information Table S2). However, the additions of NO_3^- + Fe (N + Fe) and FDW stimulated Chl *a* concentrations and PP rates to the same degree as the NO_3^- addition alone at both stations (Fig. 2; Supporting Information Table S2).

Photophysiology

Use of FRRF to interrogate phytoplankton photophysiological responses (Fm, Fv/Fm, and σ_{PSII}) to nutrient amendments demonstrated that the phytoplankton community at both sites was affected by the addition of the individual N compounds, and the response was stronger and more variable at GY than at TZ (Fig. 3). Addition of Fe alone also had a stimulating effect on PSII activity; however, N + Fe did not have an additional stimulating effect compared to NO_3^- alone.

Fm at 470 nm (Fm_{470}; inclusive of all Chl-containing plankton) increased significantly after 24 h of incubation in response to all N substrates in both experiments (Fig. 3). At TZ, all N sources resulted in a similar increase in Fm_{470} relative to the Control by 48 h. At GY, urea, NH_4^+ and N + Fe all resulted in large increases in Fm_{470} (300%) compared with the Control by 48 h, while the increase in the NO_3^- and FDW treatments was slightly less (200%). Finally, Fe addition yielded a lower but significant (Supporting Information Table S3) increase in Fm_{470} (50% relative to the Control) by 48 h at both locations.

The addition of the various N substrates also stimulated phycoerythrin-containing phytoplankton (Fm_{505}), but the responses to different N forms at the two locations varied (Fig. 3). Fm_{505} was significantly stimulated in the NO_3^- and NH_4^+ treatments by 24 h at both stations while Fm_{505} increased in response to urea only at TZ. By 48 h at TZ, NH_4^+, NO_3^-, N + Fe, and FDW additions all increased the Fm_{505} response (>130%) relative to the Control (Fig. 3b). At

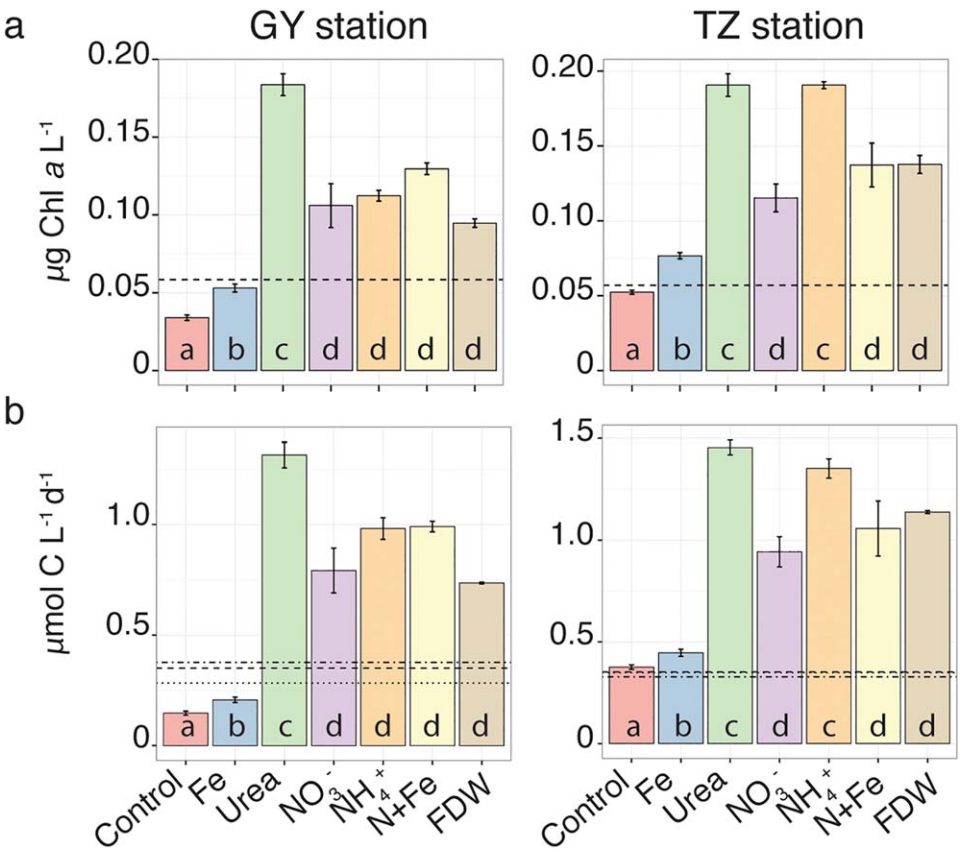

Fig. 2. Phytoplankton community responses to N compounds and Fe additions at two stations in the NPSG. (**a**) Chl *a* concentrations, (**b**) rates of ^{14}C-PP measured after 48 h of incubation at the GY and TZ stations. The significantly different means (*t*-test, $n = 3$, $p < 0.05$) are indicated with unique small letters where letter "a" indicates values not-significantly different from the control. FDW: 0.2 μm filtered 600 m deep water. The dashed lines show measurements at T0 in the control (no amendments). The dotted and dotdash lines in (**b**) show measurements at T0 in the N + Fe and FDW additions, respectively.

GY, additions of NH_4^+ and N + Fe resulted in a larger Fm_{505} response (>300% increase relative to the Control; Fig. 3b), while the responses to urea, NO_3^- and FDW were slightly less (>200% increase relative to the Control). Fe had a significant but weak effect on Fm_{505} by 48 h at both stations (Fig. 3b; Supporting Information Table S3).

Fv/Fm was significantly influenced by all N forms and by Fe largely at GY. The initial Fv/Fm_{470} was higher at the TZ station (0.51 ± 0.01 and 0.34 ± 0.02 at TZ and GY, respectively). At GY, all N additions resulted in a significant increase in Fv/Fm_{470} in comparison to the Control by 24 h, with the highest (145%) increase in response to NO_3^- and NH_4^+ (Fig. 3c). At TZ, only the NO_3^- addition resulted in a significant increase in Fv/Fm_{470} and only after 48 h (Fig. 3c; Supporting Information Table S3). Similar to Fv/Fm_{470}, the initial Fv/Fm_{505} at GY (0.41 ± 0.03) was lower than at TZ (0.50 ± 0.02). At GY, all N and Fe additions resulted in an increase in Fv/Fm_{505} similar to that of Fv/Fm_{470} (Fig. 3d). However, in contrast to responses in Fv/Fm_{470}, Fv/Fm_{505} was weakly affected by the three N forms by 24 h at TZ.

The response observed for σ_{PSII} to the additions of urea and NH_4^+ was anti-correlated with the responses observed for Chl *a* concentrations and PP. σ_{PSII} observed at 470 nm significantly decreased at TZ in response to the addition of both urea and NH_4^+ relative to the Control (Fig. 3e); in contrast, σ_{PSII} decreased only in response to urea at the GY station. Likewise, a significant decrease in response to urea was also observed for σ_{PSII} at 505 nm but only at GY (Fig. 3f; Supporting Information Table S3). A weak stimulating effect (<30% of the Control) on σ_{PSII} was observed for phytoplankton with 505 nm excitation wavelength in response to N + Fe and FDW additions at GY and in response to N + Fe and NH_4^+ at TZ (Fig. 3e,f; Supporting Information Table S3).

Responses of the phytoplankton and bacterial groups

Phytoplankton and non-photosynthetic bacteria had different qualitative and quantitative responses to N and Fe substrates, with variations depending on location.

All N forms resulted in increases in *Prochlorococcus* abundance at TZ and GY (Fig. 4a). The largest response at TZ was

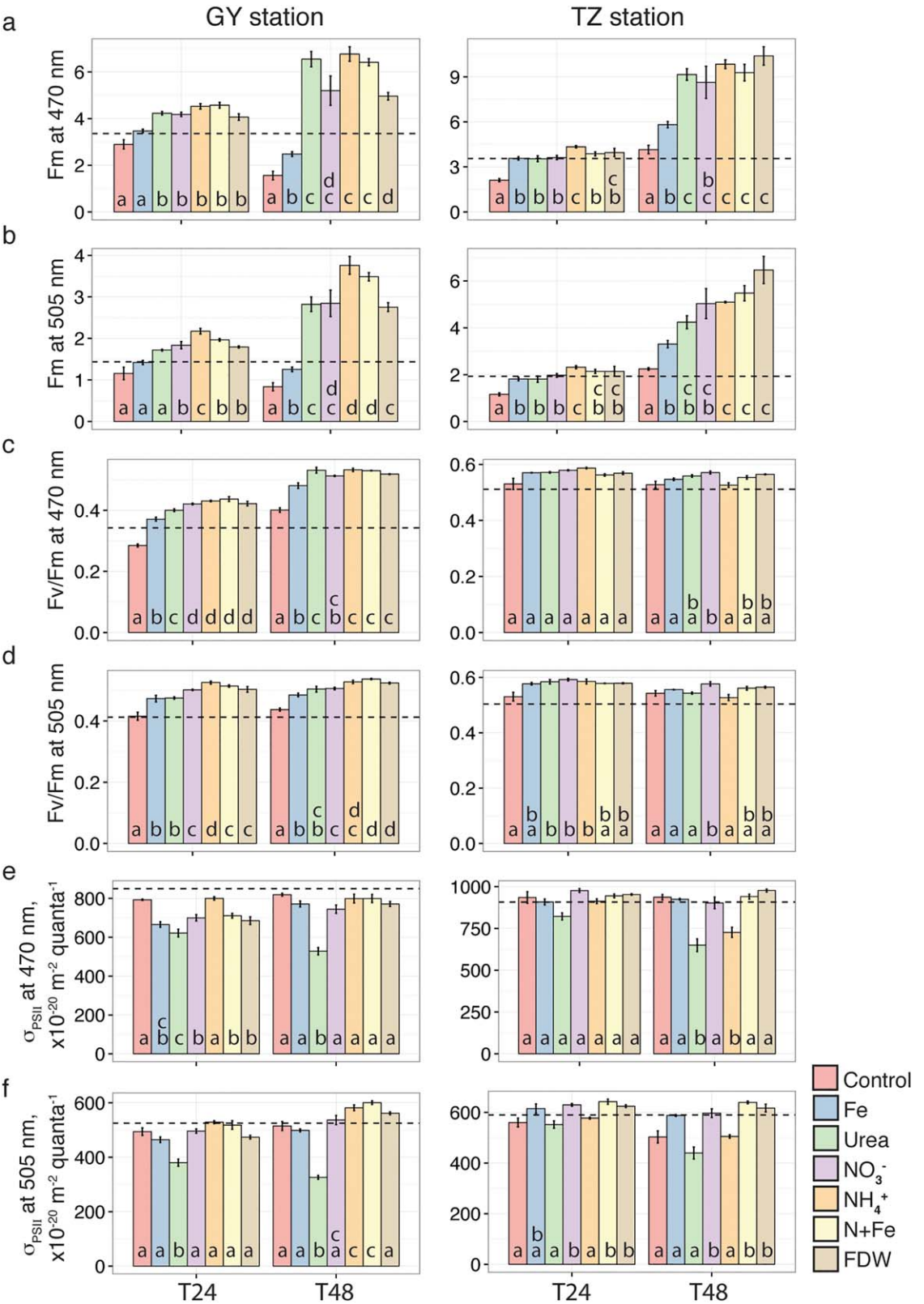

Fig. 3. Phytoplankton photosystem II physiology responses to N compounds and Fe additions in the NPSG. (**a**, **b**) Maximum in vivo fluorescence yield (Fm); (**c**, **d**) maximum photochemical efficiency of PSII (Fv/Fm); (**e**, **f**) functional absorption cross-section of PSII (σ_{PII}) measured at 470 nm (**a**, **c**, **e**) and 505 nm (**b**, **d**, **f**) excitation wavelength in response to nutrient additions at the GY and TZ stations. The dashed lines show measurements at T0. The significantly different means (*t*-test, $n = 3$, $p < 0.05$) are indicated with unique small letters where letter "a" indicates values not-significantly different from the control. FDW: 0.2 μm filtered 600 m deep water.

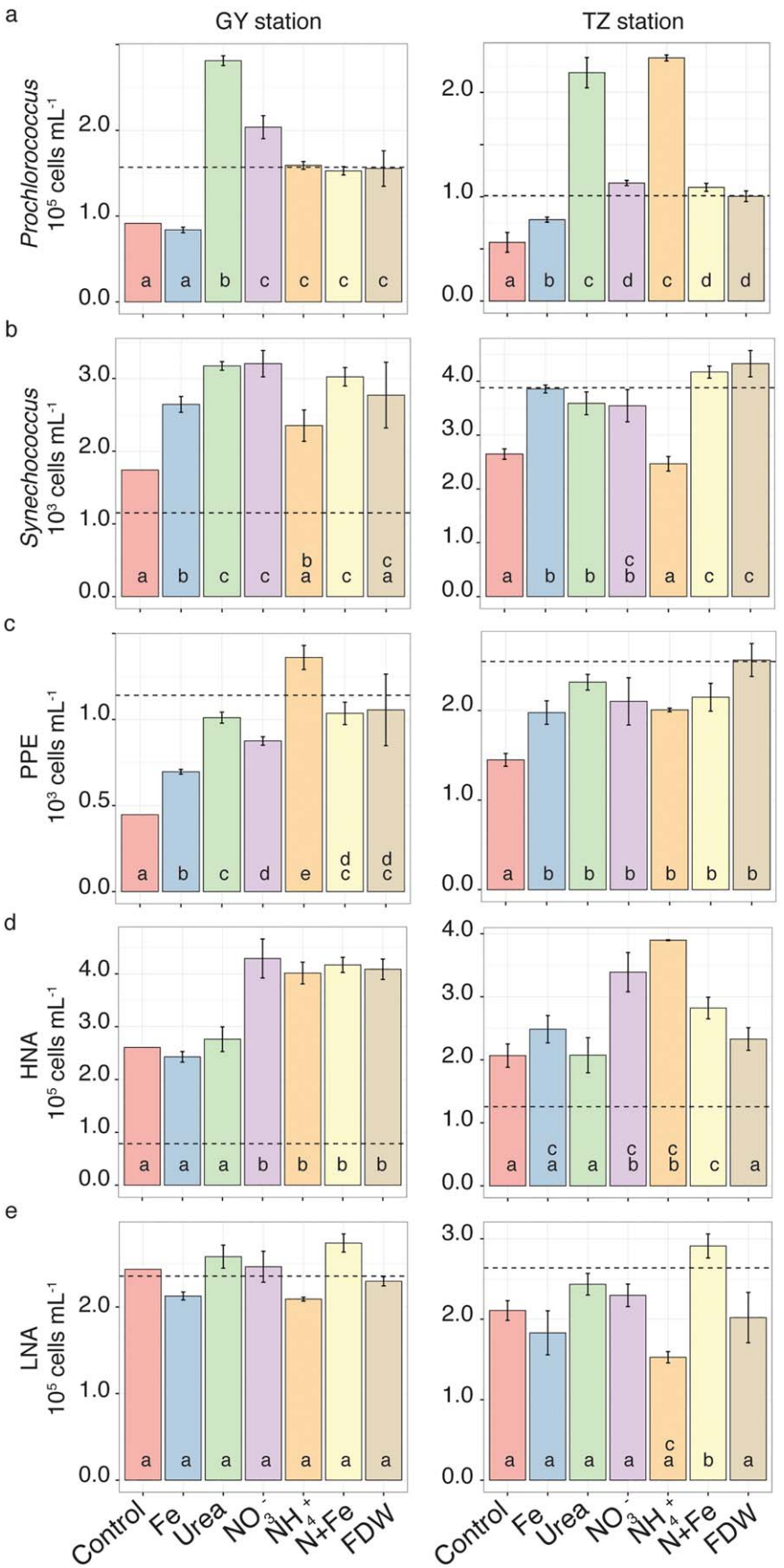

Fig. 4. Intergroup and spatial variability among phytoplankton and bacteria in responses to N compounds and Fe additions. Cell counts for (**a**) *Synechococcus*, (**b**) *Prochlorococcus*, (**c**) photosynthetic picoeukaryotes (PPE), (**d**) high nucleic acid containing bacteria (HNA) and (**e**) low nucleic acid containing bacteria (LNA) for all treatments measured 48 h after nutrient additions at the GY and TZ stations. The significantly different means (*t*-test, $n = 3$, $p < 0.05$) are indicated with unique small letters where letter "a" indicates values not-significantly different from the control. FDW: 0.2 μm filtered 600 m deep sea water.

observed in the NH_4^+ and urea treatments ($2.2 \pm 0.3\ 10^5$ cells mL^{-1}), where *Prochlorococcus* abundance was 4-times higher than in the Control after 48 h. In the NO_3^-, N + Fe, and FDW treatments, *Prochlorococcus* abundance was 2-times higher than in the Control. At GY, urea produced the largest increase in *Prochlorococcus* abundance by 48 h ($2.8 \pm 0.1 \times 10^5$ cells mL^{-1}, 3-times higher than the Control) followed by NO_3^- with 2-times higher *Prochlorococcus* abundance compared to the Control. The effects of NH_4^+, N + Fe, and FDW on *Prochlorococcus* abundances were less (~50% increase over the Control) at GY. Fe stimulated *Prochlorococcus* abundance at TZ (~40% increase over the Control) but not at GY.

Synechococcus abundance also increased significantly in response to the addition of urea, NO_3^-, N + Fe, and Fe at both stations, and the response to N was greatest at GY (Fig. 4b). *Synechococcus* abundances following the urea or NO_3^- additions were 3.5 ± 0.5 and $3.2 \pm 0.3 \times 10^3$ cells mL^{-1} (>1.3-times higher than in the Controls) at TZ and GY, respectively. Addition of NH_4^+ resulted in a decrease in *Synechococcus* abundance at TZ and only a small increase at GY; however, the effect was not significantly different from the Control by 48 h at either station (Supporting Information Table S4). *Synechococcus* abundance at both locations responded to Fe additions. While not significantly different from the effect of N at TZ, the Fe effect was significantly lower than the effects of urea and NO_3^- at GY (Supporting Information Table S4). Notably, addition of N + Fe resulted in a significantly higher *Synechococcus* response in comparison to Fe alone at both stations (Fig. 4b; Supporting Information Table S4).

PPE abundance increased significantly in response to all N forms and to Fe at both stations. Overall larger increases in PPE abundance were observed at GY (Fig. 4c) than at TZ. NO_3^- resulted in a high degree of variability between the replicates at TZ, which contributed to a lower statistical significance ($t_{(2)} = 2.4$, $p = 0.06$). PPE abundances in response to all N at TZ were ~1.5-times higher than in the Control and were similar for all nutrients including Fe (average PPE abundance in all N and Fe additions was $\sim 2.1 \pm 0.4 \times 10^3$ cells mL^{-1}). At GY by 48 h, additions of NH_4^+, urea, NO_3^-, N + Fe, and FDW resulted in >100% increases in PPE abundance relative to the Control and Fe-alone treatment (average $\sim 1.1 \pm 0.2 \times 10^3$ cells mL^{-1} in the N additions; Fig. 4c).

HNA abundance responded to additions of NH_4^+, NO_3^-, and N + Fe at both stations (up to 125% increase over the Control by 48 h, Fig. 4d). At GY, the HNA cells also increased to 1.5-times the Control in response to the FDW addition. The increase in HNA abundance at GY, but not at TZ, was significant by 24 h (Supporting Information Table S4). In contrast to the HNA cells, only the N + Fe addition at TZ station resulted in a significant increase (38% relative to the Control) in the abundance of LNA cells by 48 h (Fig. 4e). No significant increase in the LNA cell abundance was observed at GY (Fig. 4e; Supporting Information Table S4).

Shift in microbial community composition

To further evaluate the effect of N on the microbial communities at these two sites, and to assess whether differences in microbial community composition accompanied the observed changes in PP, Chl *a*, FRRF, and cell abundance, we amplified and sequenced the V3-V4 hypervariable region of the 16S rRNA gene. Based on the 16S rRNA gene relative abundances, the initial microbial community composition (Control T0) at the genus level was similar at both locations and was dominated by Cyanobacteria (genus *Prochlorococcus*, 31–34% of total 16S rRNA gene sequences) and *Alphaproteobacteria* (family *Pelagibacteraceae*, 30–33% of total 16S rRNA gene sequences), followed by other *Alphaproteobacteria* (no taxonomic assignment, 7–8% of total 16S rRNA gene sequences), *Gammaproteobacteria* (*Halomonadaceae*: *C*. Portiera, 5–7% of total 16S rRNA gene sequences), and *Actinobacteria* (*Acidimicrobiales*: OCS155, 2–3% of total 16S rRNA gene sequences) (Fig. 5a). *Synechococcus* was a minor component of the microbial community at both locations (0.7% of total 16S rRNA sequences). Relative abundances of chloroplast 16S rRNA sequences varied between the two locations. At TZ, abundances of *Haptophyceae* and *Stramenopiles* each were 1.9% of total 16S rRNA gene sequences. At GY, relative abundances of *Haptophyceae* and *Stramenopiles* in the initial community were 1.1% and 0.8%, respectively.

A shift in microbial community composition at the genus level in response to all N additions was detected within 48 h in both experiments with the strongest response to NH_4^+ (Fig. 5). Both Jaccard and Bray–Curtis ecological indices produced similar results (Fig. 5b, Supporting Information Fig. S1a). Differences in the Bray–Curtis dissimilarities between treatments were significant (difference of mean ranks between the groups $R > 0.77$, $p < 0.001$ in both experiments). At both locations, the response to all N forms was characterized by the increase in relative abundance of representatives from the *Gammaproteobacteria* families *Alteromonadaceae* and *Oceanospirillaceae* (Fig. 5a). At TZ, the relative abundance of *Alteromonadaceae* (unassigned genus) increased from 0.2% in the Control to 41%, 55%, and 57% of all reads in the urea, NH_4^+, and NO_3^- additions at T48, respectively. At GY, the relative abundance of *Alteromonadaceae* (unassigned genus) increased from 0.3% in the Control to 15%, 34%, and 36% of all reads in the urea, NO_3^-, and NH_4^+ additions at T48, respectively. Relative abundance of *Oleispira* (family *Oceanospirillaceae*) increased significantly in the N additions, but only at GY: from 0.1% in the Control to 9%, 10%, and 20% of all reads in NH_4^+, urea, and NO_3^- additions at T48, respectively. The relative abundance of another *Oceanospirillaceae* genus (*Oleibacter*) increased from undetectable in the Control to as much as 5% of all reads in the N additions at TZ. Addition of NH_4^+ resulted in the most distinct microbial community, with the shift observed within 24 h at both stations (Fig. 5a,b). Relative abundance of 16S rRNA gene sequences from representatives of the genus *Phaeobacter* (Alphaproteobacteria: *Rhodobacteraceae*) were associated

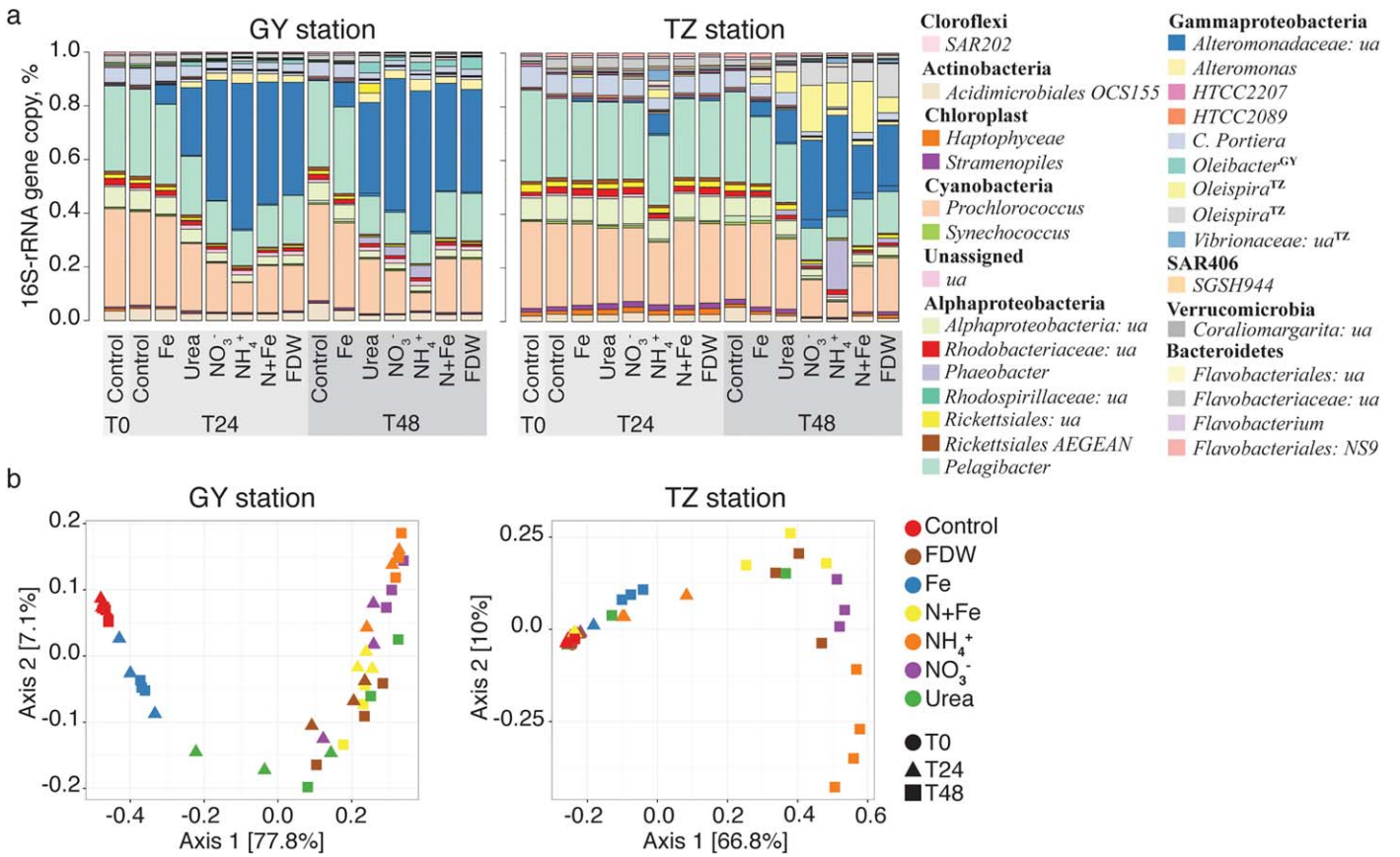

Fig. 5. Nitrogen additions resulted in a shift in microbial composition by 48 h in the NPSG. (**a**) Microbial community composition based on the relative abundance of the 16S rRNA gene copy at the genus level in the experiments at the GY and TZ stations. Only top 30 abundant genera are listed. Each sample represents a mean of 16S rRNA gene copy relative abundance from three replicates. *ua* indicates unassigned taxa. (**b**) PCoA on Bray–Curtis distance measures among the samples for heterotrophic microbial community composition at the GY and TZ stations.

with the NH_4^+ additions and increased from undetectable in the Control to 5% and 19% of all reads in the NH_4^+ addition in both GY and TZ at T48, respectively (Supporting Information Fig. S1c). Addition of urea resulted in a less pronounced change in microbial community composition, especially at TZ. Finally, Fe addition did not significantly influence community composition at both locations.

The shift in microbial community composition in response to all N forms at GY was faster than at TZ and detected by 24 h after the addition of nutrients (Fig. 5a,b). Samples taken 24 h after the start of the incubation experiment at TZ were most similar to the Controls and T0 samples. In contrast, T48 samples from treatments with any N addition at TZ clustered separately from the T0 and T24 samples, Controls, and Fe addition treatment. At GY, all of the N addition treatments clustered separately from the Controls, T0, and Fe addition within 24 h.

Response of picocyanobacteria to N

Given the great genetic diversity within marine microbial genera (e.g., Kashtan et al. 2014), we examined changes in abundance of individual taxa within *Prochlorococcus* and *Synechococcus* populations at high resolution by using an oligotyping approach (Eren et al. 2013). The responses to different N forms and Fe varied between and within *Prochlorococcus* and *Synechococcus* genera.

Prochlorococcus populations differed between the two locations (Fig. 6a). A total of 31 oligotypes were identified in *Prochlorococcus* communities across both experiments based on seven nucleotide positions with high entropy (as described in the Methods). The *Prochlorococcus* communities at TZ and GY were dominated by strains from the High Light I (HLI) and High Light II (HLII) clades, respectively. The oligotypes MED4-oligo1 (100% identical to *Prochlorococcus* MED4, HLI) and MIT9515-oligo1 (100% identical to *Prochlorococcus* MIT9515, HLI) were on average 74% and 10%, respectively, of all of the *Prochlorococcus* sequences in the Control T0 sample at TZ (Table 2). At GY, these oligotypes comprised 1% of total *Prochlorococcus* sequences in the Control T0 (Table 2). The most abundant oligotype at GY, MIT9301-oligo1 (100% identical to *Prochlorococcus* MIT9301, HLII, and strains with

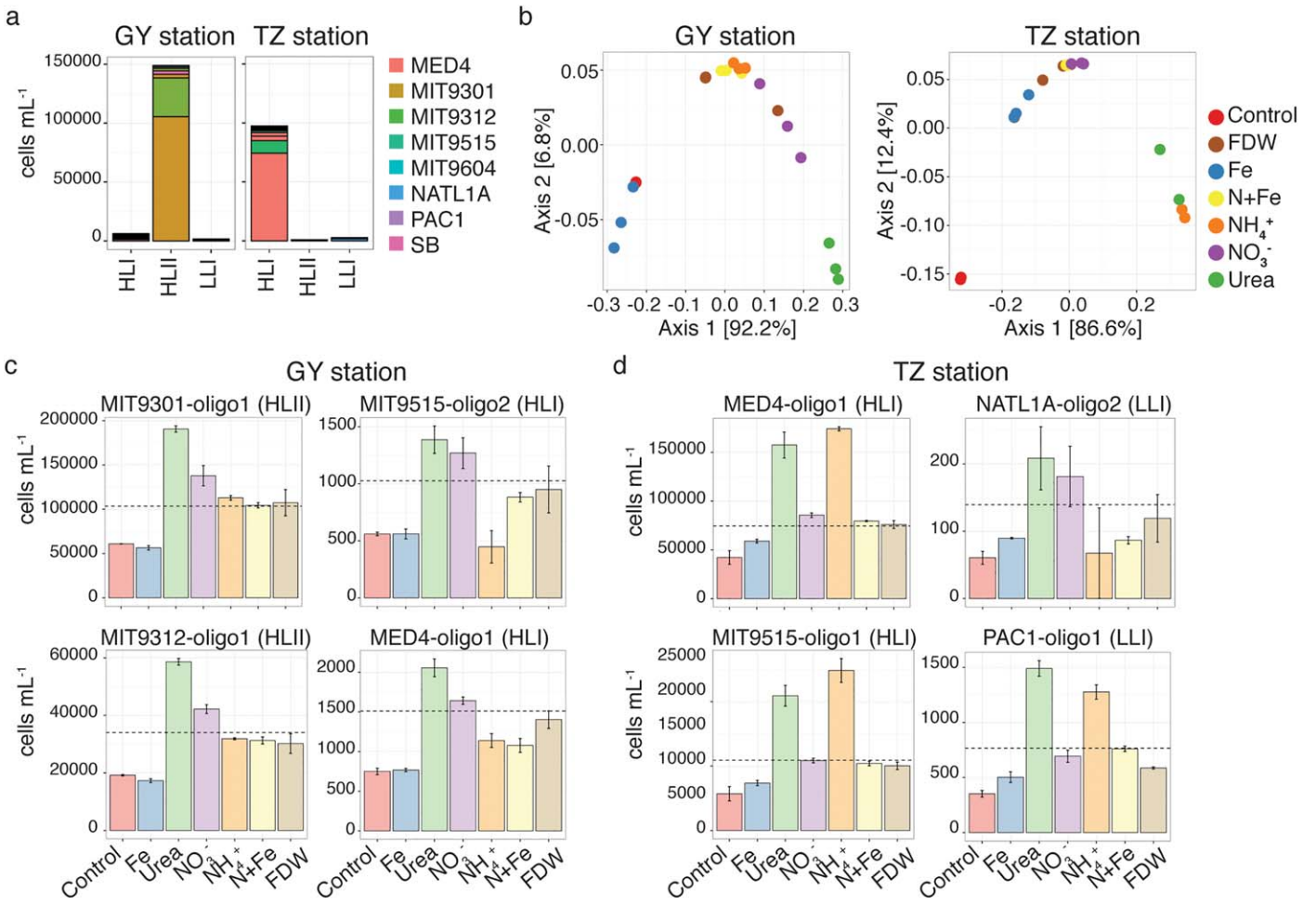

Fig. 6. Differential responses of *Prochlorococcus* oligotypes to N compounds. (**a**) Distinct *Prochlorococcus* communities were present at the GY (left panel) and TZ stations (right panel). Abundances of *Prochlorococcus* oligotypes, cells mL^{-1} (Y axis), were estimated based on 16S rRNA gene amplicon sequencing, oligotyping analysis, and cell counts. Oligotypes were assigned to Clade (X axis) and eStrain (legend) based on the highest nucleotide identity, where each eStrain represents a group of *Prochlorococcus* strains with 100% nucleotide identity in the V3-V4 region of the 16S rRNA gene sequence. (**b**) PCoA analysis on Bray–Curtis distance indices for *Prochlorococcus* community composition at T48 as a function of nutrient addition at the GY and TZ stations. (**c**, **d**) Responses in abundance of the selected *Prochlorococcus* oligotypes to nutrients at T48 at GY (**c**) and TZ (**d**). The dashed line shows abundances of each oligotype at T0.

similar sequence of the 16S rRNA gene region, Supporting Information Table S1), comprised on average 66% of the *Prochlorococcus* sequences. The next most abundant, the MIT9312-oligo1 oligotype (100% identical to *Prochlorococcus* MIT9312, HLII, and related strains, Supporting Information Table S1), was on average 22% of the *Prochlorococcus* sequences at GY station. Both of the most abundant oligotypes at GY were < 1% of the sequences in the Control T0 from TZ (Table 2). Representatives of the Low Light I (LLI) clade were present at both locations, although only as minor portions of the community (Table 2).

The addition of different N forms had differential effects on the *Prochlorococcus* populations in both experiments by 48 h (Fig. 6b–d). While urea addition resulted in a consistent increase in abundance of all *Prochlorococcus* oligotypes and clades, NH_4^+ and NO_3^- resulted in variable responses within the *Prochlorococcus* communities and between the two locations. Differences in the Bray–Curtis dissimilarities for *Prochlorococcus* communities between treatments were higher than within treatments (analysis of similarities for TZ: $R = 0.36$, $p = 0.007$, and GY: $R = 0.51$, $p = 0.002$, *see* Methods). The Bray–Curtis dissimilarity index showed that urea and NH_4^+ additions resulted in a shift in the *Prochlorococcus* community composition that was most distinct from the effects of the rest of the treatments and Controls at TZ, while the urea and NO_3^- additions resulted in the strongest shift in comparison to the effects of the rest of the treatments (and Controls) at GY (Fig. 6b). These patterns paralleled the general response of total *Prochlorococcus* abundance (measured by flow cytometry) and were observed for the most abundant

Table 2. Relative abundance and characteristics of *Prochlorococcus* and *Synechococcus* oligotypes at two experimental sites at the start of the incubation. The abundance is based on 16S rRNA gene copies and shown as percent of total 16S rRNA gene copies for each genus. Only oligotypes that contributed at least 1% to *Prochlorococcus* and *Synechococcus* populations at both sites are shown. Identity (%) shows percent nucleotide identity to the 16S rRNA gene of the closest strain(s). Score (bits) shows BLASTN score results. eStrain is a representative of a group of strains with 100% identical 16S rRNA gene V3-V4 region.

Oligotype ID	Nucleotides at high entropy positions	Nucleotide identity, %	eStrain	Clade	Relative abundance at GY, %	Relative abundance at TZ, %
Prochlorococcus						
MED4-oligo1	CGTTTCT	100	MED4	HLI	0.96	73.75
MIT9301-oligo1	TGCTAAT	100	MIT9301	HLII	66.19	0.29
MIT9312-oligo1	TACTAAT	100	MIT9312	HLII	21.64	0.45
MIT9515-oligo1	CGCTTCT	100	MIT9515	HLI	0.54	10.72
MED4-oligo2	CGTTTTT	99.75	MED4	HLI	0.55	3.75
MED4-oligo3	CGTTTAT	99.75	MED4	HLI	0.37	2.92
MIT9515-oligo2	CGCTTAT	99.75	MIT9515	HLI	0.64	1.42
SB-oligo1	TGTTAAT	100	SB	HLII	1.93	0.03
MIT9301-oligo2	TGCTTAT	99.51	MIT9301	HLII	1.91	0.04
NATL1A-oligo1	CGCTTTT	99.75	NATL1A	LLI	0.28	1.61
PAC1-oligo1	TGCTTTT	99.75	PAC1	LLI	0.85	0.76
MIT9312-oligo2	TACTTAT	99.51	MIT9312	HLII	1.26	0.01
Synechococcus						
CC9605-oligo1	ATACTCTATGC	100.00	CC9605	Clade II	61.12	34.93
CC9605-oligo2	ATACTCTATGT	99.75	CC9605	Clade II	25.46	14.09
CC9902-oligo1	ATACTCTAAGC	100.00	CC9902	Clade IV	0.00	26.30
CC9902-oligo2	ATACTCTAAGT	99.75	CC9902	Clade IV	0.00	13.64
KORDI100-oligo1	ATCCGCTCTGC	99.75	KORDI-100	Clade V	0.97	5.11
CC9605-oligo3	ATGCTCTATGC	99.75	CC9605	Clade II	5.77	0.00
CC9605-oligo4	ACACTCTATGC	99.75	CC9605	Clade II	4.34	0.34
CC9605-oligo5	ATACTCTCTGC	99.75	CC9605	Clade II	0.48	0.84
KORDI100-oligo2	ATCCGTTCTGT	99.26	KORDI-100	Clade V	0.00	1.10

Prochlorococcus oligotypes in each experiment (Fig. 6c,d). However, the minor oligotype NATL1A-oligo1 (LLI) had a larger response to urea and NO_3^- than to NH_4^+ at TZ (Fig. 6d). At GY, some members of HLII, HLI and LLI clades had no significant responses to NH_4^+ (Fig. 6c, Supporting Information Fig. S2).

Some *Prochlorococcus* oligotypes had different responses to nutrient amendments between the two sites. For example, the two dominant oligotypes at TZ, MED4-oligo1 and MIT9515-oligo1, had the greatest response to urea and NH_4^+ (Fig. 6d). However, although they were minor (<1%) components of the *Prochlorococcus* community at GY, these oligotypes had the greatest responses to urea and NO_3^- (Fig. 6c, Supporting Information Fig. S2). The responses by *Prochlorococcus* PAC1-oligo1 (LLI) also varied between the two sites (Fig. 6d, Supporting Information Fig. S2).

Similar to *Prochlorococcus*, *Synechococcus* communities at the two locations were distinct; however, the most dominant *Synechococcus* oligotypes were the same at the two locations (Fig. 7a). A total of 11 oligotypes were distinguished for *Synechococcus* based on 11 nucleotide positions with high entropy. *Synechococcus* oligotypes derived from both clades II and IV were most abundant at TZ, whereas *Synechococcus* oligotypes from clade II were most abundant at GY. *Synechococcus* oligotype CC9605-oligo1, with 100% identity to *Synechococcus* CC9605 (clade II), was the most abundant at both locations, constituting on average of 35% and 61% of *Synechococcus* 16S rRNA gene sequences at TZ and GY, respectively (Table 2). Another oligotype from clade II, CC9605-oligo2, was also present at both stations (Table 2). Two oligotypes derived from clade IV (CC9902-oligo1 and CC9902-oligo2 with 100% and 99.7% identity, respectively, to *Synechococcus* CC9902) contributed 39% to the *Synechococcus* community at TZ. The least abundant oligotypes present at both stations included representatives from clade V (Table 2).

N additions had a larger effect on *Synechococcus* community composition at GY than at TZ (Fig. 7b). Differences in the Bray–Curtis dissimilarities for *Synechococcus* communities between treatments were significantly higher than within treatments at GY (analysis of similarities for GY: $R = 0.54$, $p = 0.001$ compared to TZ: $R = 0.19$, $p = 0.07$). The Bray–Curtis dissimilarity index showed a weak separation of samples with

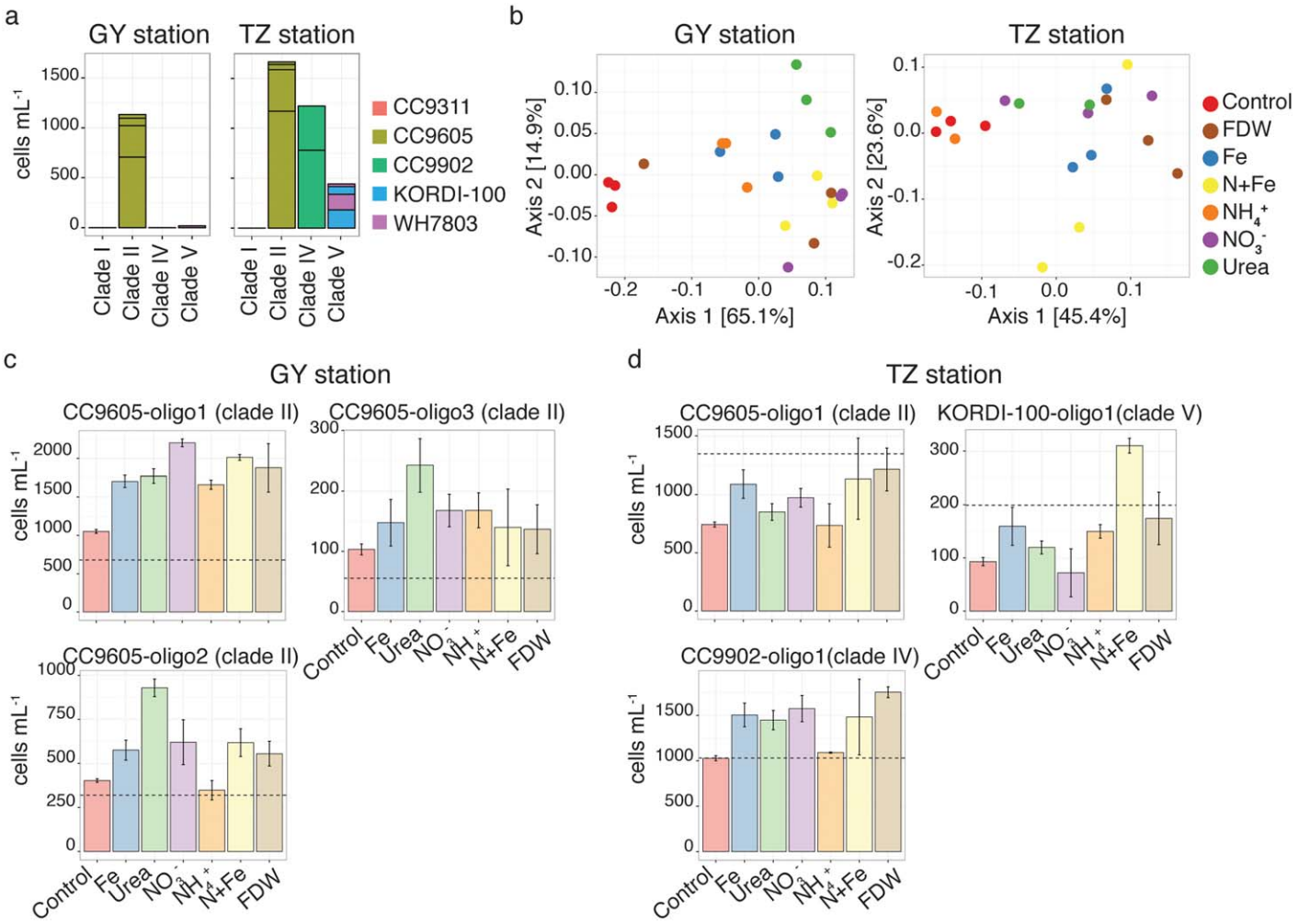

Fig. 7. Differential responses of *Synechococcus* oligotypes to N compounds. (**a**) Distinct *Synechococcus* communities were present at the GY (left panel) and TZ stations (right panel). Abundances of *Synechococcus* oligotypes, cells mL^{-1} (Y axis), were estimated based on 16S rRNA gene amplicon sequencing, oligotyping analysis, and cell counts. Oligotypes were assigned to Clade (X axis) and eStrain (legend) based on the highest nucleotide identity, where each eStrain represents a group of *Synechococcus* strains with 100% nucleotide identity in the V3-V4 region of the 16S rRNA gene sequence. (**b**) PCoA analysis on Bray–Curtis distance indices for *Synechococcus* community composition at T48 as a function of nutrient addition at the GY and TZ stations. (**c**, **d**) Responses in abundance of the selected *Synechococcus* oligotypes to nutrients at T48 at the GY (**c**) and TZ stations (**d**). The dashed line shows abundances of each oligotype at T0.

NO_3^-, urea, N + Fe, and FDW additions from the Controls and samples with NH_4^+ and Fe additions at TZ. At GY, all nutrients, including Fe, resulted in a strong shift in the *Synechococcus* community, with the urea addition resulting in the most distinct responses compared to other nutrient additions.

Similar to *Prochlorococcus*, N forms had a differential effect on *Synechococcus* oligotypes, resulting in distinct *Synechococcus* populations by 48 h (Fig. 7c,d). The response of oligotypes also varied between the sites. Consistent with the response in total *Synechococcus* abundance, the dominant oligotype CC9902-oligo1 (clade IV) responded to NO_3^-, urea, Fe, and FDW at TZ. In contrast, the oligotype CC9605-oligo5 (clade II) had a weak increase in abundance in response to urea availability relative to the Control at TZ (Fig. 7d). However, all N forms and Fe affected this oligotype abundance at GY (Fig. 7c), with the largest effect seen in the NO_3^- and N + Fe additions. Urea had the largest effect on the less abundant oligotype CC9605-oligo2 (clade II) at GY. Moreover, less abundant oligotypes had distinct responses compared to the responses of the dominant oligotypes. For example, oligotype KORDI100-oligo1 (Clade V) had a significant increase in cell abundance only in response to N + Fe at TZ (Fig. 7d), where it represented 1.1% of the *Synechococcus* community.

Discussion

The effect of N availability on biological processes in the ocean is one of the most studied topics in marine

Table 3. Responses of microbial communities to urea, NO_3^-, NH_4^+, and Fe additions in the North Pacific Ocean. The responses after 48 h are summarized for all N forms and specifically for each N substrate. Responses shared between the two stations are shown in gray and responses specific for TZ and GY stations are shown in orange and blue, respectively. The arrow up (⇑) shows an increase, and the arrow down (⇓) shows a decrease in value. Triangle (Δ) shows a shift in community composition. Reverse triangle (∇) shows consumption of a nutrient (Supporting Information Table S5). The width of arrows and size of triangles reflect the magnitude of change. The empty boxes for individual substrates/elements indicate that the response was similar to that shown in column "All N substrates." The empty boxes in the "All N substrates" indicate that the response differed among all N substrates.

Category	Measurement	All N substrates	Urea	NO_3^-	NH_4^+	Fe
Functional	Chl *a* concentrations	⇑	⇑		⇑	⇑
	^{14}C-PP rates	⇑	⇑		⇑	⇑
	Fm	⇑	⇑	⇑	⇑	⇑
	Fv/Fm	⇑	⇑	⇑	⇑	⇑
	σ_{PSII}		⇓		⇓	
Taxonomic I: cell count	*Prochlorococcus*	⇑	⇑		⇑	
	Synechococcus		⇑	⇑		⇑
	PPE	⇑				⇑
	HNA cells			⇑	⇑	
Taxonomic II: community composition based on 16S rRNA gene	Heterotrophic microbial community	Δ		Δ	Δ	Δ
	Prochlorococcus	Δ	Δ	Δ	Δ	Δ
	Synechococcus		Δ	Δ	Δ	
Nutrient consumption	N substrate	∇			∇	
	PO_4^{3-}	∇			∇	∇

microbiology; however, we still know little about the complex interactions between the diverse microbial communities and different N compounds used by specific microorganisms. We investigated the effects of NO_3^-, NH_4^+, and urea as sources of N on microbial community activity (PP and photosynthetic efficiency), and community composition (based on major microbial group cell counts and 16S rRNA gene sequence) in the open ocean waters of the North Pacific Ocean. All N forms tested had significant effects on microbial communities at the investigated sites in the NPSG within 48 h (Table 3). Limitation of PP and maximum photochemical efficiency of PSII by N has been reported in other low-latitude oligotrophic waters, such as in the North Atlantic Ocean (Graziano et al. 1996; Moore et al. 2008; Davey et al. 2008). Moreover, N was the major limiting nutrient constraining total phytoplankton biomass in the Western South Pacific Ocean (Moisander et al. 2012) and in the South Pacific Gyre (Van Wambeke et al. 2008). In addition to N, either P or Fe can co-limit picoplankton cell growth in the North Atlantic (Davey et al. 2008). While the effect of SRP was not specifically tested in our study, the addition of FDW (which had elevated SRP and NO_3^- concentrations, Table 1) resulted in similar responses as the addition of N alone, suggesting that P did not co-limit plankton biomass or productivity during our experiments.

Stimulating effect of urea on phytoplankton

The importance of urea as an N source for phytoplankton was demonstrated decades ago (McCarthy 1972*b*; Price and Harrison 1988; Antia et al. 1991; Fan et al. 2003). The urease gene has been found in a variety of marine microorganisms, including the cyanobacteria *Synechococcus* and *Prochlorococcus*, eukaryotic phytoplankton (haptophytes, diatoms, prasinophytes), and heterotrophic bacteria (*Roseobacteraceae*, *Pelagibacter*, Gammaproteobacteria HTCC2207) (Baker et al. 2009; Collier et al. 2009; Solomon et al. 2010). Urea concentrations in the surface open oceans appear highly variable in space and time, ranging from 0.3 μmol N L^{-1} to 0.7 μmol N

L^{-1} (Bronk 2002; Painter et al. 2008). In the current study, urea was added at much higher concentrations (2.5 μmol of N L^{-1} and 5.0 μmol of N L^{-1}) than previously reported *in situ* however, our results demonstrated that all major groups of phytoplankton responded to the urea additions, with responses differing between the two locations examined (Table 3). Previous studies have also described variable responses in rates of N uptake and growth in phytoplankton when urea was supplied as the sole N source (Cochlan and Harrison 1991; Lomas and Glibert 2000; Moore et al. 2002; Fan et al. 2003; Solomon et al. 2010).

Our results suggest that urea may be an important N source for *Prochlorococcus* (Figs. 6, 7), which is responsible for a large fraction of PP in the open oceans (Vaulot et al. 1995; Campbell et al. 1997; DuRand et al. 2001). *Prochlorococcus* clades HLI and HLII dominated at the TZ and GY stations, respectively, consistent with the observations that these clades occupy different niches, with the shift from the HLI to the HLII clade reported at the threshold of ~23°C in summer (Farrant et al. 2016; Larkin et al. 2016). *Prochlorococcus* HLI and HLII are the most abundant *Prochlorococcus* clades (Johnson et al. 2006) and the majority of sequenced *Prochlorococcus* genomes have urea utilization and transporter genes (Kettler et al. 2007; Scanlan et al. 2009). The results of our study showed that both clades responded significantly to urea additions, demonstrating large increases in abundance, >300% relative to the Controls. The oligotyping analysis of *Prochlorococcus* 16S rRNA gene sequences further showed that *Prochlorococcus* community composition was strongly influenced by urea additions at both sites. The high transcription of the urea transporter gene in natural populations of *Prochlorococcus* found in metatranscriptomic studies (Frias-Lopez et al. 2008; Gifford et al. 2011; Shi et al. 2011) suggests that *Prochlorococcus* actively acquire urea. Indeed, rates of urea uptake by *Prochlorococcus* in the Sargasso Sea were found to be similar or faster than NH_4^+ uptake rates (Casey et al. 2007), and a significant relationship was observed between *Prochloroccocus* abundances and bulk urea uptake rates in the Northern Atlantic Ocean (Painter et al. 2008). While utilization of urea by picocyanobacteria has been shown before (Rippka et al. 2000; Moore et al. 2002), our study suggests that urea may be an important source of N supporting the growth of natural populations of *Prochlorococcus*.

Variable responses of phytoplankton to NH_4^+ and NO_3^-

In contrast to urea, the effects of NO_3^- and NH_4^+ on phytoplankton communities varied between the sites. The addition of NH_4^+ significantly stimulated rates of PP both at the TZ and GY stations. At GY, both NO_3^- and NH_4^+ additions resulted in a similar degree of enhancement in PP, but responses to these additions had a less stimulating effect than that of urea. The PP response pattern at TZ was paralleled by changes in *Prochlorococcus* cell abundance and community composition. The different responses to the two N forms were likely the result of uptake preferences by different phytoplankton groups for NO_3^- and NH_4^+, as well as different degrees of Fe limitation experienced among the phytoplankton groups at TZ (discussed below).

Genetic and physiological differences may help explain the differential responses of *Prochlorococcus* populations to NH_4^+ and NO_3^- between the two experimental sites. Genes encoding pathways for NO_3^-/NO_2^- assimilation have been found in some *Prochlorococcus* HL and LL strains, and these strains are able to grow solely on NO_3^- as an N source (Martiny et al. 2009; Berube et al. 2015). Thus, not surprisingly, naturally occurring *Prochlorococcus* populations from HLI, HLII, and LLI clades responded to NO_3^- additions at low NH_4^+ concentrations at both stations in our study. Laboratory studies indicate that *Prochlorococcus* growth on NO_3^- is slower than growth on NH_4^+ (Berube et al. 2015) and such results could explain the differences in cell abundances in response to NO_3^- and NH_4^+ additions at TZ. Additionally, the genome of *Prochlorococcus* MIT9515 (HLI), a strain that was abundant at TZ, has two copies of the *amt* gene which encodes an NH_4^+ transporter (Scanlan et al. 2009) and this strain may be more competitive for NH_4^+ than the strains that were present at the GY station. In contrast, the genome of *Prochlorococcus* MIT0604 (HLII, with the V3-V4 region of the 16S rRNA gene sequence 100% identical to *Prochlorococcus* MIT9301, the eStrain that was dominant at GY) has two clusters of NO_3^- assimilation genes (Berube et al. 2015). Finally, another HLII strain (SB strain) present at GY has the most extensive gene suite for N utilization, including NO_3^-, urea, and cyanate assimilation genes (Berube et al. 2015). In addition to the genetic and physiological differences, microbial interactions likely influenced the observed changes in abundance. For example, it is possible that NO_3^- additions may have stimulated growth of mixotrophic eukaryotes that consumed *Prochlorococcus* cells (Hartmann et al. 2013). In general, the N-limitation of *Prochlorococcus* cell abundance observed in the present study contrasted with results observed in the Western South Pacific Ocean where *Prochlorococcus* HLII responded to Fe and P (Moisander et al. 2012), a finding that may reflect lower N : Fe or N : P supply ratios in the northern hemisphere (Ward et al. 2013).

It was surprising that *Synechococcus* abundance showed little response to the NH_4^+ addition. NH_4^+ is thought to be the preferred N substrate by cyanobacteria over NO_3^- because of the higher energetic cost for reduction and assimilation of NO_3^-. However, culture studies showed that under subsaturating irradiance, growth rates of marine *Synechococcus* on NO_3^- were similar to growth rates on NH_4^+ (Collier et al. 2012). Considering that *Prochlorococcus* and heterotrophic bacteria were orders of magnitude more abundant than *Synechococcus* at both stations, and that *Synechococcus* cells have a lower surface area to volume ratio than *Prochlorococcus* (Morel et al. 1993), *Synechococcus* may have been at a

competitive disadvantage for NH_4^+ uptake. However, the fact that ~50% of the added NH_4^+ remained after 48 h of incubation (Supporting Information Table S5) suggests that *Synechococcus* preferred NO_3^- as an N source, although the mechanism for N substrate preference remains unclear (Collier et al. 2012).

In contrast to *Synechococcus*, the photosynthetic picoeukaryotes showed the greatest increase in abundance in the NH_4^+ addition, but only at GY. The lack of a PPE response to NH_4^+ at TZ may be related to Fe availability (see below). A preference for NH_4^+ over NO_3^- and urea has been previously shown for PPEs in culture, such as the prasinophyte *Micromonas* (Cochlan and Harrison 1991). Interestingly, the prasinophytes *Micromonas* and *Ostreococcus* have genes for two types of NH_4^+ transporter (AMT), one of which is similar to bacterial *amt* (Derelle et al. 2006; McDonald et al. 2010). Transcription of this AMT gene is up-regulated in response to N-depletion (McDonald et al. 2010). Likewise, transcription of the NH_4^+ transporter genes in response to N-depletion has also been shown for diatoms (Allen 2005; Bowler et al. 2008). The data presented here support the observations of previous studies that eukaryotic phytoplankton can successfully compete for NH_4^+ with smaller bacterial cells (Bradley et al. 2010).

Fe limitation of phytoplankton growth and activity in the CCS

Fe availability affected the abundance of all groups of phytoplankton and rates of PP at TZ. Fe limitation of phytoplankton growth in the CCS is believed to be due to the rapid depletion of Fe relative to NO_3^- in the upwelled waters that travel offshore as filaments (Bruland et al. 2001; Biller and Bruland 2013). In addition, the TZ site was in an anticyclonic eddy containing open ocean water with relatively high SRP, but otherwise low nutrient and Chl *a* concentrations. The mixing of open ocean water at the sampling site is further supported by the mixture of coastal and open ocean phytoplankton communities found at this site. For example, the coastal *Synechococcus* clade IV, usually prevalent in colder nutrient-rich waters, was present at the same abundance as *Synechococcus* clade II, which is the dominant open ocean clade (Sohm et al. 2016). The high abundance of *Prochlorococcus* at this site also indicated an input of oligotrophic gyre waters. Thus, the mixing of the oligotrophic gyre waters at TZ may have contributed to the low Fe availability.

The genetic differences between the communities at the two stations is likely an additional factor contributing to the stronger response to Fe at TZ. For example, coastal strains of phytoplankton are adapted to have higher cellular Fe quotas than open ocean strains (Brand 1991; Sunda et al. 1991; Strzepek and Harrison 2004). Moreover, *Prochlorococcus* MED4 (HLI), which was abundant at TZ, has been shown to be especially sensitive to Fe availability (Thompson et al. 2011). Finally, *Prochlorococcus* has a larger number of genes for coping with low Fe environments than *Synechococcus* (Rocap et al. 2003; Scanlan et al. 2009), which may explain why *Prochlorococcus* had a greater response to N than to Fe additions, in contrast to *Synechococcus* at TZ. Thus, a combination of factors, genetic and environmental, may have resulted in the strong community response to Fe at TZ. These results provide further support for Fe limitation of phytoplankton growth in the CCS transition zone.

Furthermore, some microbial populations were most likely N and Fe co-limited at TZ. An independent type of co-limitation of biomass (Arrigo 2005; Saito et al. 2008) may explain why the addition of N and Fe together did not enhance the response in Chl *a* and primary productivity relative to N or Fe additions alone. If only a small fraction of the community are N and Fe co-limited in comparison to the N-limited fraction, then the effect of N + Fe may not be significant in bulk measurements. The responses by the *Synechococcus* oligotypes support this hypothesis: The oligotype identical to *Synechococcus* KORDI-100 (clade V) had greater relative abundances in N + Fe in comparison to the Fe or N additions alone. However, this oligotype comprised only 5% of the total *Synechococcus* population, and thus did not contribute significantly to the responses in total *Synechococcus* biomass. The two other *Synechococcus* oligotypes at TZ (originating from clades II and IV) showed similar responses to N + Fe, Fe, or NO_3^-. These were the most abundant *Synechococcus* oligotypes at TZ and likely comprised many subpopulations that could not be distinguished at the 16S rRNA gene resolution. Thus, using the high resolution oligotyping approach allowed us to distinguish the diversity of responses within microbial populations, such as to nutrient co-limitation, which were not reflected in the bulk measurements.

Responses of heterotrophic microbial communities to N substrates

The heterotrophic community responded to N forms differently than the phototrophic community. The NH_4^+ followed by the NO_3^- additions at both locations resulted in the strongest shifts in heterotrophic community composition, as estimated from 16S rRNA gene relative abundances (Table 3). Additionally, HNA cell abundances increased in the NO_3^- and NH_4^+ additions at both sites regardless of the phytoplankton response (Table 3). The shift was largely due to the increase in the relative abundance of Gammaproteobacteria (*Oceanospirillaceae*, *Alteromonadaceae*, and *Vibrionaceae*) and Alphaproteobacteria (*Phaeobacter*), the copiotrophic microbial taxa known to respond rapidly to enrichments of surface seawater with nutrients or associated with phytoplankton blooms (González et al. 2000; Shi et al. 2012; Beier et al. 2015; El-Swais et al. 2015; Sosa et al. 2015). Smaller in size than some phytoplankton cells in general, heterotrophic bacteria may have a competitive advantage by taking up available NH_4^+ and NO_3^- rapidly, thereby actively competing

for macronutrients, as has been reported in many other studies (Eppley et al. 1977; Wheeler and Kirchman 1986; Kirchman 1994; Mills et al. 2008; Bradley et al. 2010).

Differences between the TZ and GY stations

The greatest differences in microbial community responses to N additions between the two locations were in the timing and degree of the responses. The shift in heterotrophic microbial community composition at GY was observed earlier than at TZ. This may be due to the distinct phototrophic communities at each location. For example, *Prochlorococcus* HLI and *Synechococcus* Clades II and IV were dominant at TZ, and *Prochlorococcus* HLII and *Synechococcus* Clade II were dominant at GY. However, our study suggests that the microbial community was under more severe nutrient limitation at GY than at TZ. The nutricline at GY was deeper than at TZ, and the microbes at GY had likely been nutrient limited longer than those at the TZ station. The low initial Fv/Fm of the phototrophic community at GY and the significant and rapid (in 24 h) increase in Fv/Fm upon N additions suggest that new N contributed to the building of new photosynthetic proteins and that photosynthetic activity at GY was strongly N-limited (Suggett et al. 2009). The increase in PP following N additions was also significantly greater at GY than at TZ. As previously shown in cultures, N pre-conditioning affects how fast phytoplankton respond to N (Conway et al. 1976; Price and Harrison 1988). Additionally, phytoplankton species have the ability to change substrate affinities and uptake potentials depending on the degree of nutrient limitation (Conway and Harrison 1977). Thus, microbial community composition and N preconditioning may determine the timing and degree of the responses to N substrates in the North Pacific.

Conclusions

N substrates have differential effects on different phytoplankton groups, and the degree and rapidity of the responses depend on the pre-existing physicochemical conditions (e.g., Price and Harrison 1988). Our study extends previous findings by using a combination of techniques to measure total microbial community physiological and functional responses as well as shifts in microbial community composition and changes in abundance of phytoplankton populations at high taxonomic resolution. The results of our study indicate that N availability limited PP and accumulation of microbial biomass during our sampling in the open ocean waters of the North Pacific. Moreover, we observed distinct differences in rates of PP, accumulation of biomass, and community composition in response to additions of urea, NH_4^+, and NO_3^-. The growth of some populations of phytoplankton, especially *Synechococcus* and PPE, was also limited by Fe in the CCS region. Our results also suggest the heterotrophic microbial community successfully competed for inorganic N sources at both experimental sites. Finally, besides the differences in community composition, the pre-existing conditions at each site likely influenced the timing and degree of the responses to N perturbations by both phytoplankton and heterotrophic community.

There is strong evidence that future oceans will experience changes in temperature and N supply (Kim et al. 2014). The genetics of populations determines how environmental factors affect their ecologies and evolution (e.g., Larkin et al. 2016), and the results of our study imply that changes in N substrate availability favors different components of the phytoplankton community in different oceanic regions. More importantly, because phytoplankton taxa vary in elemental stoichiometry (Sterner and Elser 2002; Bertilsson et al. 2003; Heldal et al. 2003), physiology (e.g., Moore et al. 2002), viral resistance (Stoddard et al. 2007) and DOM production (Becker et al. 2014), changes in phytoplankton community composition would impact biogeochemical cycles, as well as ecological processes. The results of our study underline the importance of better understanding the complex interactions between diverse microbial populations and nutrient availability in the oceans.

References

Allen, A. E. 2005. Beyond sequence homology: Redundant ammonium transporters in a marine diatom are not functionally equivalent. J. Phycol. **41**: 4–6. doi:10.1111/j.0022-3646.2005.41101_2.x

Allen, A. E., G. Booth, M. E. Frischer, P. G. Verity, J. P. Zehr, and S. Zani. 2001. Diversity and detection of nitrate assimilation genes in marine bacteria. Appl. Environ. Microbiol. **67**: 5343–5348. doi:10.1128/AEM.67.11.5343-5348.2001

Allen, A. E., A. Vardi, and C. Bowler. 2006. An ecological and evolutionary context for integrated nitrogen metabolism and related signaling pathways in marine diatoms. Curr. Opin. Plant Biol. **9**: 264–273. doi:10.1016/j.pbi.2006.03.013

Altschul, S. F., W. Gish, W. Miller, E. W. Myers, and D. J. Lipman. 1990. Basic local alignment search tool. J. Mol. Biol. **215**: 403–410. doi:10.1016/S0022-2836(05)80360-2

Aluwihare, L. I., and T. Meador. 2008. Chemical composition of marine dissolved organic nitrogen, p. 95–140. *In* D. G. Capone, D. A. Bronk, M. R. Mulholland, and E. J. Carpenter [eds.], Nitrogen in the marine environment, 2nd ed. Elsevier Academic Press.

Antia, N. J., J. Harrison, and L. Oliveira. 1991. The role of dissolved organic nitrogen in phytoplankton nutrition, cell biology and ecology. Phycologia **30**: 1–89. doi:10.2216/i0031-8884-30-1-1.1

Arrigo, K. R. 2005. Marine microorganisms and global nutrient cycles. Nature **437**: 349–355. doi:10.1038/nature04159

Baker, K. M., J. Gobler, and J. L. Collier. 2009. Urease gene sequences from algae and heterotrophic bacteria in axenic and nonaxenic phytoplankton cultures. J. Phycol. **45**: 625–634. doi:10.1111/j.1529-8817.2009.00680.x

Becker, J. W., P. M. Berube, C. L. Follett, J. B. Waterbury, S. W. Chisholm, E. F. Delong, and D. J. Repeta. 2014. Closely related phytoplankton species produce similar suites of dissolved organic matter. Front. Microbiol. **5**: 14. doi:10.3389/fmicb.2014.00111

Beier, S., A. R. Rivers, M. A. Moran, and I. Obernosterer. 2015. The transcriptional response of prokaryotes to phytoplankton-derived dissolved organic matter in seawater. Environ. Microbiol. **17**: 3466–3480. doi:10.1111/1462-2920.12434

Bertilsson, S., O. Berglund, D. M. Karl, and S. W. Chisholm. 2003. Elemental composition of marine *Prochlorococcus* and *Synechococcus*: Implications for the ecological stoichiometry of the sea. Limnol. Oceanogr. **48**: 1721–1731. doi:10.4319/lo.2003.48.5.1721

Berube, P. M., and others. 2015. Physiology and evolution of nitrate acquisition in *Prochlorococcus*. ISME J. **9**: 1195–1207. doi:10.1038/ismej.2014.211

Bidigare, R. R. 1983. Nitrogen excretion by marine zooplankton, p. 385–409. *In* E. J. Carpenter and D. G. Capone [eds.], Nitrogen in the marine environment. Academic Press.

Biller, D. V., and K. W. Bruland. 2013. Sources and distributions of Mn, Fe, Co, Ni, Cu, Zn, and Cd relative to macronutrients along the central California coast during the spring and summer upwelling season. Mar. Chem. **155**: 50–70. doi:10.1016/j.marchem.2013.06.003

Biller, D. V., and K. W. Bruland. 2014. The central California Current transition zone: A broad region exhibiting evidence for iron limitation. Prog. Oceanogr. **120**: 370–382. doi:10.1016/j.pocean.2013.11.002

Bonnet, S., and others. 2008. Nutrient limitation of primary productivity in the Southeast Pacific (BIOSOPE cruise). Biogeosciences **5**: 215–225. doi:10.5194/bg-5-215-2008

Böttjer, D., J. E. Dore, D. M. Karl, R. M. Letelier, C. Mahaffey, S. T. Wilson, and M. J. Church. 2016. Temporal variability in nitrogen fixation and particulate nitrogen export at Station ALOHA. Limnol. Oceanogr. **62**: 200–216. doi:10.1002/lno.10386

Bowler, C., and others. 2008. The *Phaeodactylum* genome reveals the evolutionary history of diatom genomes. Nature **456**: 239–244. doi:10.1038/nature07410

Bradley, P. B., M. P. Sanderson, M. E. Frischer, J. Brofft, M. G. Booth, L. J. Kerkhof, and D. A. Bronk. 2010. Inorganic and organic nitrogen uptake by phytoplankton and heterotrophic bacteria in the stratified Mid-Atlantic Bight. Estuar. Coast. Shelf Sci. **88**: 429–441. doi:10.1016/j.ecss.2010.02.001

Brand, L. E. 1991. Minimum iron requirements of marine-phytoplankton and the implications for the biogeochemical control of new production. Limnol. Oceanogr. **36**: 1756–1771. doi:10.4319/lo.1991.36.8.1756

Bronk, D. A. 2002. Dynamics of DON, p. 153–247. In D. A. Hansell and C. A. Carlson [eds.], Biogeochemistry of marine dissolved organic matter. Academic Press.

Bronk, D. A., M. Glibert, T. C. Malone, S. Banahan, and E. Sahlsten. 1998. Inorganic and organic nitrogen cycling in Chesapeake Bay: Autotrophic versus heterotrophic processes and relationships to carbon flux. Aquat. Microb. Ecol. **15**: 177–189. doi:10.3354/ame015177

Bruland, K. W., L. Rue, and G. J. Smith. 2001. Iron and macronutrients in California coastal upwelling regimes: Implications for diatom blooms. Limnol. Oceanogr. **46**: 1661–1674. doi:10.4319/lo.2001.46.7.1661

Campbell, L., H. B. Liu, H. A. Nolla, and D. Vaulot. 1997. Annual variability of phytoplankton and bacteria in the subtropical North Pacific Ocean at Station ALOHA during the 1991-1994 ENSO event. Deep-Sea Res. Part I **44**: 167–192. doi:10.1016/S0967-0637(96)00102-1

Caporaso, J. G., and others. 2010. QIIME allows analysis of high-throughput community sequencing data. Nat. Methods **7**: 335–336. doi:10.1038/nmeth.f.303

Capotondi, A., M. A. Alexander, N. A. Bond, E. N. Curchitser, and J. D. Scott. 2012. Enhanced upper ocean stratification with climate change in the CMIP3 models. J. Geophys. Res. **117**: C04031. doi:10.1029/2011JC007409

Casey, J. R., W. Lomas, J. Mandecki, and D. E. Walker. 2007. *Prochlorococcus* contributes to new production in the Sargasso Sea deep chlorophyll maximum. Geophys. Res. Lett. **34**: L10604. doi:10.1029/2006GL028725

Chisholm, S. W., J. Olson, E. R. Zettler, R. Goericke, J. B. Waterbury, and N. A. Welschmeyer. 1988. A novel free-living prochlorophyte abundant in the oceanic euphotic zone. Nature **334**: 340–343. doi:10.1038/334340a0

Cochlan, W. P., and P. J. Harrison. 1991. Uptake of nitrate, ammonium, and urea by nitrogen-starved cultures of *Micromonas-pusilla* (*Prasinophyceae*) - transient responses. J. Phycol. **27**: 673–679. doi:10.1111/j.0022-3646.1991.00673.x

Collier, J. L., M. Baker, and S. L. Bell. 2009. Diversity of urea-degrading microorganisms in open-ocean and estuarine planktonic communities. Environ. Microbiol. **11**: 3118–3131. doi:10.1111/j.1462-2920.2009.02016.x

Collier, J. L., R. Lovindeer, Y. Xi, J. C. Radway, and R. A. Armstrong. 2012. Differences in growth and physiology of marine *Synechococcus* (Cyanobacteria) on nitrate versus ammonium are not determined solely by nitrogen source redox state. J. Phycol. **48**: 106–116. doi:10.1111/j.1529-8817.2011.01100.x

Conway, H. L., J. Harrison, and C. O. Davis. 1976. Marine diatoms grown in chemostats under silicate or ammonium limitation. 2. Transient-response of *Skeletonema-costatum* to a single addition of limiting nutrient. Mar. Biol. **35**: 187–199. doi:10.1007/BF00390940

Conway, H. L., and P. J. Harrison. 1977. Marine diatoms grown in chemostats under silicate or ammonium limitation. 4. Transient-response of *Chaetoceros-debilis, Skeletonema-costatum*, and *Thalassiosira-gravida* to a single addition of limiting nutrient. Mar. Biol. **43**: 33–43. doi:10.1007/BF00392569

Corner, E. D. S., and B. S. Newell. 1967. On nutrition and metabolism of zooplankton. 4. Forms of nitrogen excreted by *Calanus*. J. Mar. Biol. Assoc. U. K. **47**: 113–120. doi:10.1017/S0025315400033609

Davey, M., G. A. Tarran, M. M. Mills, C. Ridame, R. J. Geider, and J. LaRoche. 2008. Nutrient limitation of picophytoplankton photosynthesis and growth in the tropical North Atlantic. Limnol. Oceanogr. **53**: 1722–1733. doi:10.4319/lo.2008.53.5.1722

Derelle, E., and others. 2006. Genome analysis of the smallest free-living eukaryote *Ostreococcus tauri* unveils many unique features. Proc. Natl. Acad. Sci. USA **103**: 11647–11652. doi:10.1073/pnas.0604795103

DeSantis, T. Z., and others. 2006. Greengenes, a chimera-checked 16S rRNA gene database and workbench compatible with ARB. Appl. Environ. Microbiol. **72**: 5069–5072. doi:10.1128/AEM.03006-05

Dore, J. E., and D. M. Karl. 1996. Nitrification in the euphotic zone as a source for nitrite, nitrate, and nitrous oxide at Station ALOHA. Limnol. Oceanogr. **41**: 1619–1628. doi:10.4319/lo.1996.41.8.1619

Dore, J. E., T. Houlihan, D. V. Hebel, G. Tien, L. Tupas, and D. M. Karl. 1996. Freezing as a method of sample preservation for the analysis of dissolved inorganic nutrients in seawater. Mar. Chem. **53**: 173–185. doi:10.1016/0304-4203(96)00004-7

Duce, R. A., and others. 2008. Impacts of atmospheric anthropogenic nitrogen on the open ocean. Science **320**: 893–897. doi:10.1126/science.1150369

Dugdale, R. C., and J. J. Goering. 1967. Uptake of new and regenerated forms of nitrogen in primary productivity. Limnol. Oceanogr. **12**: 196–206. doi:10.4319/lo.1967.12.2.0196

DuRand, M. D., J. Olson, and S. W. Chisholm. 2001. Phytoplankton population dynamics at the Bermuda Atlantic Time-series station in the Sargasso Sea. Deep-Sea Res. Part II **48**: 1983–2003. doi:10.1016/S0967-0645(00)00166-1

Edgar, R. C. 2010. Search and clustering orders of magnitude faster than BLAST. Bioinformatics **26**: 2460–2461. doi:10.1093/bioinformatics/btq461

El-Swais, H., K. A. Dunn, J. P. Bielawski, W. K. W. Li, and D. A. Walsh. 2015. Seasonal assemblages and short-lived blooms incoastal north-west Atlantic Ocean bacterioplankton. Environ. Microbiol. **17**: 3642–3661. doi:10.1111/1462-2920.12629

Eppley, R. W., H. Sharp, E. H. Renger, M. J. Perry, and W. G. Harrison. 1977. Nitrogen assimilation by phytoplankton and other microorganisms in surface waters of central North Pacific Ocean. Mar. Biol. **39**: 111–120. doi:10.1007/BF00386996

Eppley, R. W., and B. J. Peterson. 1979. Particulate organic-matter flux and planktonic new production in the deep ocean. Nature **282**: 677–680. doi:10.1038/282677a0

Eren, A. M., L. Maignien, W. J. Sul, L. G. Murphy, S. L. Grim, H. G. Morrison, and M. L. Sogin. 2013. Oligotyping: Differentiating between closely related microbial taxa using 16S rRNA gene data. Methods Ecol. Evol. **4**: 1111–1119. doi:10.1111/2041-210X.12114

Fan, C., P. M. Glibert, J. Alexander, and M. W. Lomas. 2003. Characterization of urease activity in three marine phytoplankton species, *Aureococcus anophagefferens, Prorocentrum minimum*, and *Thalassiosira weissflogii*. Mar. Biol. **142**: 949–958. doi:10.1007/s00227-003-1017-8

Farrant, G. K., and others. 2016. Delineating ecologically significant taxonomic units from global patterns of marine picocyanobacteria. Proc. Natl. Acad. Sci. USA **113**: E3365–E3374. doi:10.1073/pnas.1524865113

Fawcett, S. E., M. Lomas, J. R. Casey, B. B. Ward, and D. M. Sigman. 2011. Assimilation of upwelled nitrate by small eukaryotes in the Sargasso Sea. Nat. Geosci. **4**: 717–722. doi:10.1038/ngeo1265

Frias-Lopez, J., Y. Shi, G. W. Tyson, M. L. Coleman, S. C. Schuster, S. W. Chisholm, and E. F. Delong. 2008. Microbial community gene expression in ocean surface waters. Proc. Natl. Acad. Sci. USA **105**: 3805–3810. doi:10.1073/pnas.0708897105

Garside, C. 1982. A chemi-luminescent technique for the determination of nanomolar concentrations of nitrate and nitrite in sea-water. Mar. Chem. **11**: 159–167. doi:10.1016/0304-4203(82)90039-1

Gifford, S. M., S. Sharma, J. M. Rinta-Kanto, and M. A. Moran. 2011. Quantitative analysis of a deeply sequenced marine microbial metatranscriptome. ISME J. **5**: 461–472. doi:10.1038/ismej.2010.141

González, J. M., R. Simó, R. Massana, J. S. Covert, E. O. Casamayor, C. Pedrós-Alió, and M. A. Moran. 2000. Bacterial community structure associated with a dimethylsulfoniopropionate-producing North Atlantic algal bloom. Appl. Environ. Microbiol. **66**: 4237–4246. doi:10.1128/AEM.66.10.4237-4246.2000

Graziano, L. M., J. Geider, W. K. W. Li, and M. Olaizola. 1996. Nitrogen limitation of North Atlantic phytoplankton: Analysis of physiological condition in nutrient enrichment experiments. Aquat. Microb. Ecol. **11**: 53–64. doi:10.3354/ame011053

Green, S. J., R. Venkatramanan, and A. Naqib. 2015. Deconstructing the Polymerase Chain Reaction: Understanding and correcting bias associated with primer degeneracies and primer-template mismatches. PLoS One **10**: 21. doi:10.1371/journal.pone.0128122

Gruber, N., and J. N. Galloway. 2008. An Earth-system perspective of the global nitrogen cycle. Nature **451**: 293–296. doi:10.1038/nature06592

Hallam, S. J., T. J. Mincer, C. Schleper, C. M. Preston, K. Roberts, P. M. Richardson, and E. F. DeLong. 2006. Pathways of carbon assimilation and ammonia oxidation suggested by environmental genomic analyses of marine *Crenarchaeota*. PLoS Biol. **4**: 520–536. doi:10.1371/journal.pbio.0040095

Hansell, D. A., and J. J. Goering. 1989. A method for estimating uptake and production-rates for urea in seawater using

[^{14}C] urea and [^{15}N] urea. Can. J. Fish. Aquat. Sci. **46**: 198–202. doi:10.1139/f89-027

Hartmann, M., M. V. Zubkov, D. J. Scanlan, and C. Lepere. 2013. In situ interactions between photosynthetic picoeukaryotes and bacterioplankton in the Atlantic Ocean: Evidence for mixotrophy. Environ. Microbiol. Rep. **5**: 835–840. doi:10.1111/1758-2229.12084

Heldal, M., D. J. Scanlan, S. Norland, F. Thingstad, and N. H. Mann. 2003. Elemental composition of single cells of various strains of marine *Prochlorococcus* and *Synechococcus* using X-ray microanalysis. Limnol. Oceanogr. **48**: 1732–1743. doi:10.4319/lo.2003.48.5.1732

Herlemann, D. P. R., M. Labrenz, K. Jurgens, S. Bertilsson, J. J. Waniek, and A. F. Andersson. 2011. Transitions in bacterial communities along the 2000 km salinity gradient of the Baltic Sea. ISME J. **5**: 1571–1579. doi:10.1038/ismej.2011.41

Johnson, Z. I., R. Zinser, A. Coe, N. P. McNulty, E. M. S. Woodward, and S. W. Chisholm. 2006. Niche partitioning among *Prochlorococcus* ecotypes along ocean-scale environmental gradients. Science **311**: 1737–1740. doi:10.1126/science.1118052

Karner, M. B., F. DeLong, and D. M. Karl. 2001. Archaeal dominance in the mesopelagic zone of the Pacific Ocean. Nature **409**: 507–510. doi:10.1038/35054051

Kashtan, N., and others. 2014. Single-cell genomics reveals hundreds of coexisting subpopulations in wild *Prochlorococcus*. Science **344**: 416–420. doi:10.1126/science.1248575

Kettler, G. C., and others. 2007. Patterns and implications of gene gain and loss in the evolution of *Prochlorococcus*. PLoS Genet. **3**: 2515–2528. doi:10.1371/journal.pgen.0030231

Kim, I. N., K. Lee, N. Gruber, D. M. Karl, J. L. Bullister, S. Yang, and T.-W. Kim. 2014. Increasing anthropogenic nitrogen in the North Pacific Ocean. Science **346**: 1102–1106. doi:10.1126/science.1258396

Kirchman, D. L. 1994. The uptake of inorganic nutrients by heterotrophic bacteria. Microbiol. Ecol. **28**: 255–271. doi:10.1007/BF00166816

Kolber, Z. S., O. Prasil, and P. G. Falkowski. 1998. Measurements of variable chlorophyll fluorescence using fast repetition rate techniques: Defining methodology and experimental protocols. Biochim. Biophys. Acta **1367**: 88–106. doi:10.1016/S0005-2728(98)00135-2

Larkin, A. A., S. K. Blinebry, C. Howes, Y. Lin, S. E. Loftus, C. A. Schmaus, E. R. Zinser, and Z. I. Johnson. 2016. Niche partitioning and biogeography of high light adapted *Prochlorococcus* across taxonomic ranks in the North Pacific. ISME J. **10**: 1555–1567. doi:10.1038/ismej.2015.244

Li, Q. P., Z. Zhang, F. J. Millero, and D. A. Hansell. 2005. Continuous colorimetric determination of trace ammonium in seawater with a long-path liquid waveguide capillary cell. Mar. Chem. **96**: 73–85. doi:10.1016/j.marchem.2004.12.001

Lomas, M. W., and P. M. Glibert. 2000. Comparisons of nitrate uptake, storage, and reduction in marine diatoms and flagellates. J. Phycol. **36**: 903–913. doi:10.1046/j.1529-8817.2000.99029.x

Marie, D., F. Partensky, D. Vaulot, and C. Brussaard. 1999. Enumeration of phytoplankton, bacteria, and viruses in marine samples, p. 11.11.1–11.11.15. *In* J. P. Robinson [ed.], Current protocols in cytometry. John Wiley and Sons.

Martiny, A. C., S. Kathuria, and P. M. Berube. 2009. Widespread metabolic potential for nitrite and nitrate assimilation among *Prochlorococcus* ecotypes. Proc. Natl. Acad. Sci. USA **106**: 10787–10792. doi:10.1073/pnas.0902532106

Mayzaud, P. 1973. Respiration and nitrogen excretion of zooplankton. 2. Studies of metabolic characteristics of starved animals. Mar. Biol. **21**: 19–28. doi:10.1007/BF00351188

McCarthy, J. J. 1972*a*. Uptake of urea by marine phytoplankton. J. Phycol. **8**: 216–222. doi:10.1111/j.1529-8817.1972.tb04031.x

McCarthy, J. J. 1972*b*. Uptake of urea by natural populations of marine phytoplankton. Limnol. Oceanogr. **17**: 738–748. doi:10.4319/lo.1972.17.5.0738

McDonald, S. M., J. N. Plant, and A. Z. Worden. 2010. The mixed lineage nature of nitrogen transport and assimilation in marine eukaryotic phytoplankton: A case study of *Micromonas*. Mol. Biol. Evol. **27**: 2268–2283. doi:10.1093/molbev/msq113

McMurdie, P. J., and S. Holmes. 2013. phyloseq: An R package for reproducible interactive analysis and graphics of microbiome census data. PLoS One **8**: 11. doi:10.1371/journal.pone.0061217

Mills, M. M., C. Ridame, M. Davey, J. La Roche, and R. J. Geider. 2004. Iron and phosphorus co-limit nitrogen fixation in the eastern tropical North Atlantic. Nature **429**: 292–294. doi:10.1038/nature02550

Mills, M. M., and others. 2008. Nitrogen and phosphorus co-limitation of bacterial productivity and growth in the oligotrophic subtropical North Atlantic. Limnol. Oceanogr. **53**: 824–834. doi:10.4319/lo.2008.53.2.0824

Mitamura, O., and Y. Saijo. 1981. Studies on the seasonal-changes of dissolved organic-carbon, nitrogen, phosphorus and urea concentrations in lake Biwa. Arch. Hydrobiol. **91**: 1–14.

Moisander, P. H., A. Beinart, M. Voss, and J. P. Zehr. 2008. Diversity and abundance of diazotrophic microorganisms in the South China Sea during intermonsoon. ISME J. **2**: 954–967. doi:10.1038/ismej.2008.51

Moisander, P. H., F. Zhang, E. A. Boyle, I. Hewson, J. P. Montoya, and J. P. Zehr. 2012. Analogous nutrient limitations in unicellular diazotrophs and *Prochlorococcus* in the South Pacific Ocean. ISME J. **6**: 733–744. doi:10.1038/ismej.2011.152

Montoya, J. P., J. Carpenter, and D. G. Capone. 2002. Nitrogen fixation and nitrogen isotope abundances in zooplankton of the oligotrophic North Atlantic. Limnol. Oceanogr. **47**: 1617–1628. doi:10.4319/lo.2002.47.6.1617

Moonsamy, P. V., and others. 2013. High throughput HLA genotyping using 454 sequencing and the Fluidigm Access Array (TM) system for simplified amplicon library preparation. Tissue Antigens **81**: 141–149. doi:10.1111/tan.12071

Moore, C. M., M. M. Mills, R. Langlois, A. Milne, E. P. Achterberg, J. La Roche, and R. J. Geider. 2008. Relative influence of nitrogen and phosphorus availability on phytoplankton physiology and productivity in the oligotrophic sub-tropical North Atlantic Ocean. Limnol. Oceanogr. **53**: 291–305. doi:10.4319/lo.2008.53.1.0291

Moore, C. M., and others. 2013. Processes and patterns of oceanic nutrient limitation. Nat. Geosci. **6**: 701–710. doi:10.1038/ngeo1765

Moore, L. R., F. Post, G. Rocap, and S. W. Chisholm. 2002. Utilization of different nitrogen sources by the marine cyanobacteria *Prochlorococcus* and *Synechococcus*. Limnol. Oceanogr. **47**: 989–996. doi:10.4319/lo.2002.47.4.0989

Morel, A., Y. H. Ahn, F. Partensky, D. Vaulot, and H. Claustre. 1993. *Prochlorococcus* and *Synechococcus* - a comparative-study of their optical-properties in relation to their size and pigmentation. J. Mar. Res. **51**: 617–649. doi:10.1357/0022240933223963

Morris, R. M., M. S. Rappé, S. A. Connon, K. L. Vergin, W. A. Siebold, C. A. Carlson, and S. J. Giovannoni. 2002. SAR11 clade dominates ocean surface bacterioplankton communities. Nature **420**: 806–810. doi:10.1038/nature01240

Mulholland, M. R., and M. W. Lomas. 2008. Nitrogen uptake and assimilation, p. 303–384. In D. G. Capone, D. A. Bronk, M. R. Mulholland, and E. J. Carpenter [eds.], Nitrogen in the marine environment, 2nd ed. Elsevier Academic Press.

Obata, H., H. Karatani, and E. Nakayama. 1993. Automated-determination of iron in seawater by chelating resin concentration and chemiluminescence detection. Anal. Chem. **65**: 1524–1528. doi:10.1021/ac00059a007

Oksanen, J., and others. 2016. vegan: Community ecology package. R package version 2.4-1. Available from https://CRAN.R-project.org/package=vegan

Ortega-Retuerta, E., W. H. Jeffrey, J. F. Ghiglione, and F. Joux. 2012. Evidence of heterotrophic prokaryotic activity limitation by nitrogen in the Western Arctic Ocean during summer. Polar Biol. **35**: 785–794. doi:10.1007/s00300-011-1109-8

Painter, S. C., R. Sanders, H. N. Waldron, M. I. Lucas, and S. Torres-Valdés. 2008. Urea distribution and uptake in the Atlantic Ocean between 50° N and 50° S. Mar. Ecol.-Prog. Ser. **368**: 53–63. doi:10.3354/meps07586

Price, N. M., and P. J. Harrison. 1988. Urea uptake by Sargasso Sea phytoplankton - saturated and in situ uptake rates. Deep-Sea Res. Part II **35**: 1579–1593. doi:10.1016/0198-0149(88)90104-5

R Core Team. 2013. R: A language and environment for statistical computing. R Foundation for Statistical Computing, Vienna, Austria. URL http://www.R-project.org/

Quay, P. D., C. Peacock, K. Björkman, and D. M. Karl. 2010. Measuring primary production rates in the ocean: Enigmatic results between incubation and non-incubation methods at Station ALOHA. Global Biogeochem. Cycles **24**: GB3014. doi:10.1029/2009GB003665

Rippka, R., and others. 2000. *Prochlorococcus marinus* Chisholm et al. 1992 subsp pastoris subsp nov strain PCC 9511, the first axenic chlorophyll a(2)/b(2)-containing cyanobacterium (Oxyphotobacteria). Int. J. Syst. Evol. Microbiol. **50**: 1833–1847. doi:10.1099/00207713-50-5-1833

Rocap, G., and others. 2003. Genome divergence in two *Prochlorococcus* ecotypes reflects oceanic niche differentiation. Nature **424**: 1042–1047. doi:10.1038/nature01947

Sahlsten, E. 1987. Nitrogenous nutrition in the euphotic zone of the central North Pacific Gyre. Mar. Biol. **96**: 433–439. doi:10.1007/BF00412528

Saito, M. A., J. Goepfert, and J. T. Ritt. 2008. Some thoughts on the concept of colimitation: Three definitions and the importance of bioavailability. Limnol. Oceanogr. **53**: 276–290. doi:10.4319/lo.2008.53.1.0276

Scanlan, D. J., and others. 2009. Ecological genomics of marine picocyanobacteria. Microbiol. Mol. Biol. Rev. **73**: 249–299. doi:10.1128/MMBR.00035-08

Shi, Y. M., W. Tyson, J. M. Eppley, and E. F. DeLong. 2011. Integrated metatranscriptomic and metagenomic analyses of stratified microbial assemblages in the open ocean. ISME J. **5**: 999–1013. doi:10.1038/ismej.2010.189

Shi, Y. M., J. McCarren, and E. F. DeLong. 2012. Transcriptional responses of surface water marinemicrobial assemblages to deep-sea water amendment. Environ. Microbiol. **14**: 191–206. doi:10.1111/j.1462-2920.2011.02598.x

Sohm, J. A., N. A. Ahlgren, Z. J. Thomson, C. Williams, J. W. Moffett, M. A. Saito, E. A. Webb, and G. Rocap. 2016. Co-occurring *Synechococcus* ecotypes occupy four major oceanic regimes defined by temperature, macronutrients and iron. ISME J. **10**: 333–345. doi:10.1038/ismej.2015.115

Solomon, C. M., L. Collier, G. M. Berg, and P. M. Glibert. 2010. Role of urea in microbial metabolism in aquatic systems: A biochemical and molecular review. Aquat. Microb. Ecol. **59**: 67–88. doi:10.3354/ame01390

Sosa, O. A., M. Gifford, D. J. Repeta, and E. F. DeLong. 2015. High molecular weight dissolved organic matter enrichment selects for methylotrophs in dilution to extinction cultures. ISME J. **9**: 2725–2739. doi:10.1038/ismej.2015.68

Steeman-Nielsen, E. 1952. The use of radioactive carbon (C14) for measuring organic production in the sea. J. Cons. Int. Explor. Mer. **18**: 117–140. doi:10.1093/icesjms/18.2.117

Sterner, R. W., and J. J. Elser. 2002. Ecological stoichiometry: The biology of elements from molecules to biosphere. Princeton Univ. Press.

Stoddard, L. I., B. H. Martiny, and M. F. Marston. 2007. Selection and characterization of cyanophage resistance

in marine *Synechococcus* strains. Appl. Environ. Microbiol. **73**: 5516–5522. doi:10.1128/AEM.00356-07

Strickland, J. D. H., and T. R. Parsons. 1972. A practical handbook of seawater analysis, 2nd ed. Fisheries Research Board of Canada, Bulletin 167.

Strzepek, R. F., and P. J. Harrison. 2004. Photosynthetic architecture differs in coastal and oceanic diatoms. Nature **431**: 689–692. doi:10.1038/nature02954

Suggett, D. J., M. Moore, A. E. Hickman, and R. J. Geider. 2009. Interpretation of fast repetition rate (FRR) fluorescence: Signatures of phytoplankton community structure versus physiological state. Mar. Ecol. Prog. Ser. **376**: 1–19. doi:10.3354/meps07830

Sunda, W. G., G. Swift, and S. A. Huntsman. 1991. Low iron requirement for growth in oceanic phytoplankton. Nature **351**: 55–57. doi:10.1038/351055a0

Thompson, A. W., K. Huang, M. A. Saito, and S. W. Chisholm. 2011. Transcriptome response of high- and low-light-adapted *Prochlorococcus* strains to changing iron availability. ISME J. **5**: 1580–1594. doi:10.1038/ismej.2011.49

Van Wambeke, F., S. Bonnet, T. Moutin, P. Raimbault, G. Alarcon, and C. Guieu. 2008. Factors limiting heterotrophic bacterial production in the southern Pacific Ocean. Biogeosciences **5**: 833–845. doi:10.5194/bg-5-833-2008

Vaulot, D., D. Marie, R. J. Olson, and S. W. Chisholm. 1995. Growth of *Prochlorococcus*, a photosynthetic prokaryote, in the equatorial pacific-ocean. Science **268**: 1480–1482. doi:10.1126/science.268.5216.1480

Ward, B. A., S. Dutkiewicz, C. M. Moore, and M. J. Follows. 2013. Iron, phosphorus, and nitrogen supply ratios define the biogeography of nitrogen fixation. Limnol. Oceanogr. **58**: 2059–2075. doi:10.4319/lo.2013.58.6.2059

Waterbury, J. B., W. Watson, R. R. L. Guillard, and L. E. Brand. 1979. Widespread occurrence of a unicellular, marine, planktonic cyanobacterium. Nature **277**: 293–294. doi:10.1038/277293a0

Welschmeyer, N. A. 1994. Fluorometric analysis of chlorophyll-*a* in the presence of chlorophyll-*b* and pheopigments. Limnol. Oceanogr. **39**: 1985–1992. doi:10.4319/lo.1994.39.8.1985

Wheeler, P. A., and D. L. Kirchman. 1986. Utilization of inorganic and organic nitrogen by bacteria in marine systems. Limnol. Oceanogr. **31**: 998–1009. doi:10.4319/lo.1986.31.5.0998

Wickham, H. 2009. ggplot2: Elegant graphics for data analysis. Springer-Verlag New York.

Worden, A. Z., K. Nolan, and B. Palenik. 2004. Assessing the dynamics and ecology of marine picophytoplankton: The importance of the eukaryotic component. Limnol. Oceanogr. **49**: 168–179. doi:10.4319/lo.2004.49.1.0168

Yool, A., A. P. Martin, C. Fernandez, and D. R. Clark. 2007. The significance of nitrification for oceanic new production. Nature **447**: 999–1002. doi:10.1038/nature05885

Zehr, J. P., and R. M. Kudela. 2011. Nitrogen cycle of the open ocean: From genes to ecosystems. Ann. Rev. Mar. Sci. **3**: 197–225. doi:10.1146/annurev-marine-120709-142819

Zhang, J. J., K. Kobert, T. Flouri, and A. Stamatakis. 2014. PEAR: A fast and accurate Illumina Paired-End reAd mergeR. Bioinformatics **30**: 614–620. doi:10.1093/bioinformatics/btt593

Zhu, Y., D. X. Yuan, Y. M. Huang, J. Ma, S. C. Feng, and K. N. Lin. 2014. A modified method for on-line determination of trace ammonium in seawater with a long-path liquid waveguide capillary cell and spectrophotometric detection. Mar. Chem. **162**: 114–121. doi:10.1016/j.marchem.2014.03.011

Acknowledgments

We thank the captain, crew and technicians of the R/V *New Horizon* for assistance and support during the research cruise. We thank Mary Hogan (UCSC) for helping in preparations for the cruises and DNA extraction, Joaquin Pampin Baro (GEOMAR) for providing support for the trace-metal free work, Dr. Stefan Green and his staff at the DNA Services Facility (the University of Illinois, Chicago) for next generation sequencing consultation, Ed Boring (UCSC) for bioinformatics assistance. In addition, Susan Curless, Brenner Wai, Alexa Nelson, and Stu Goldberg all provided laboratory support of this project. This work was supported by awards from the National Science Foundation Dimensions in Biodiversity program (OCE 1241221), Center for Microbial Oceanography: Research and Education (NSF EF0424599), and the Deutsche Forschungsgemeinschaft as part of Sonderforschungsbereich 754: 'Climate-Biogeochemistry Interactions in the Tropical Ocean' (to EPA).

Conflict of Interest

None declared.

Submitted 02 September 2016
Revised 20 February 2017
Accepted 07 April 2017

Associate editor: Anya Waite